ANNUAL REVIEWS

Annual Review of Biophysics

The Effects of Temperature on Cellular Physiology

Benjamin D. Knapp[1] and Kerwyn Casey Huang[1,2,3,4]

[1]Biophysics Program, Stanford University School of Medicine, Stanford, California, USA; email: kchuang@stanford.edu

[2]Department of Bioengineering, Stanford University, Stanford, California, USA

[3]Department of Microbiology and Immunology, Stanford University School of Medicine, Stanford, California, USA

[4]Chan Zuckerberg Biohub, San Francisco, California, USA

Annu. Rev. Biophys. 2022. 51:499–526

The *Annual Review of Biophysics* is online at biophys.annualreviews.org

https://doi.org/10.1146/annurev-biophys-112221-074832

Keywords

Arrhenius law, enzymes, growth, central dogma, membrane fluidity, physiology, microbial ecology, global warming

Abstract

Temperature impacts biological systems across all length and timescales. Cells and the enzymes that comprise them respond to temperature fluctuations on short timescales, and temperature can affect protein folding, the molecular composition of cells, and volume expansion. Entire ecosystems exhibit temperature-dependent behaviors, and global warming threatens to disrupt thermal homeostasis in microbes that are important for human and planetary health. Intriguingly, the growth rate of most species follows the Arrhenius law of equilibrium thermodynamics, with an activation energy similar to that of individual enzymes but with maximal growth rates and over temperature ranges that are species specific. In this review, we discuss how the temperature dependence of critical cellular processes, such as the central dogma and membrane fluidity, contributes to the temperature dependence of growth. We conclude with a discussion of adaptation to temperature shifts and the effects of temperature on evolution and on the properties of microbial ecosystems.

Contents

INTRODUCTION

Rising global temperatures and accumulating evidence that temperature shapes microbial ecosystems (18, 61) have prompted a resurgence of interest in general aspects of temperature sensitivity across all kingdoms (59, 61). Due to their inability to regulate intracellular temperature, microorganisms are particularly susceptible to temperature changes, as increased temperatures increase enzymatic rates, thereby enhancing growth, but also cause denaturation that threatens function. Environmental microorganisms, which are critical for global nutrient cycling (18), must be able to tolerate sudden (e.g., weather-related), diurnal, and seasonal variations in temperature while also evolving on geological timescales and in response to anthropogenic climate change. The observation that runoff from water-cooled industrial and power facilities into natural aquatic systems increased the likelihood of bacterial infections in fish prompted early concerns about thermal pollution (97). Temperature is the largest contributing factor to microbial composition in the world's oceans (144), and increased soil temperatures decrease microbial biomass and increase carbon loss (93). Host–microbe interactions can also depend strongly on temperature. For example, the 1927 Nobel Prize in Medicine was awarded for the discovery that fever treatment (pyrotherapy) could successfully treat neurosyphilis (162); in addition, fungal infections in mammals are rare, thought to be due in part to inhospitably high host temperatures (approximately 37°C) (17). These connections with planetary and human health motivate the search for a deeper, systems-level understanding of how temperature affects cellular growth.

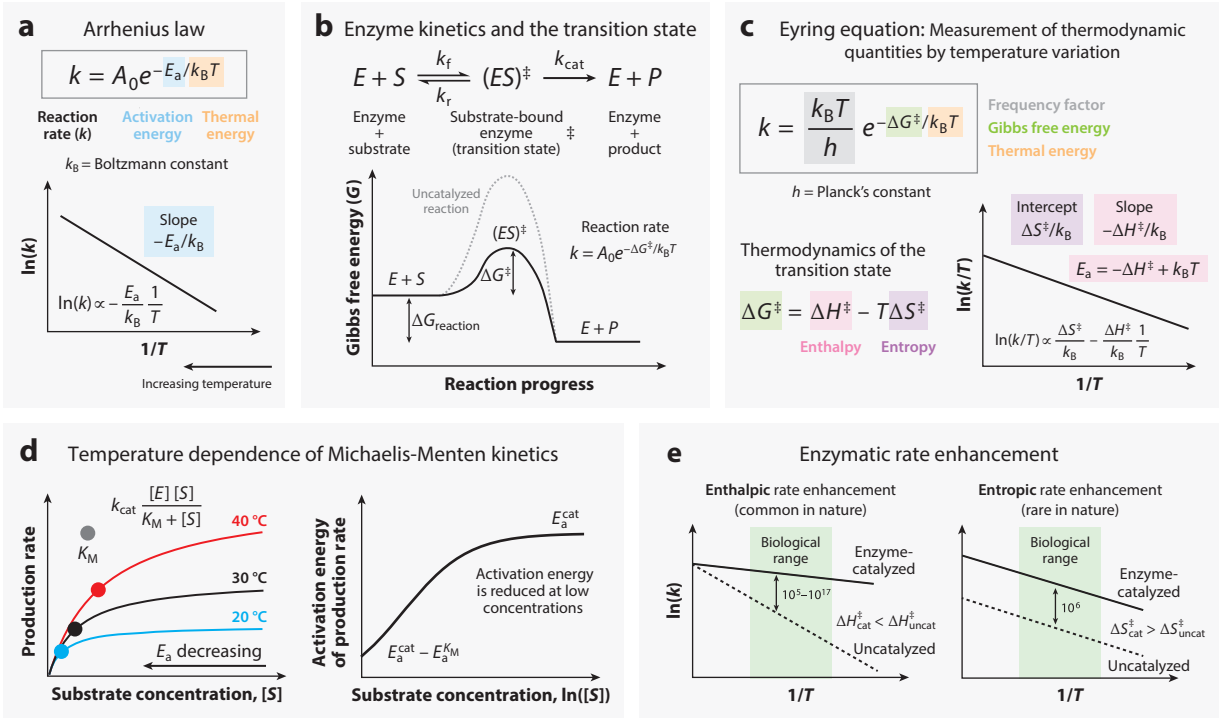

Figure 1

The effects of temperature on enzyme kinetics. (*a*) The Arrhenius law from equilibrium thermodynamics describes the empirical observation that the logarithm of the rate of a chemical reaction, ln(*k*), depends linearly on the inverse absolute temperature (*T*). The slope of this relationship is the activation energy (E_a). (*b*) In classical enzyme kinetic theory, an enzyme (*E*) binds reversibly (forward rate k_f, reverse rate k_r) to a substrate (*S*) to form a transition state ($ES^{\ddagger}$) that irreversibly catalyzes the formation of product (*P*) at the catalytic rate, k_{cat}. The enzyme effectively lowers the free energy barrier of the transition state ($\Delta G^{\ddagger}$) for the reaction. (*c*) The Eyring equation derived from transition state theory relates the rate of a chemical reaction (*k*) exponentially to the change in Gibbs free energy at the transition state ($\Delta G^{\ddagger}$). The frequency factor ($k_B T/h$) captures the contribution of thermal vibrations. Fitting of ln(k/T) versus $1/T$ provides a measurement of the activation enthalpy ($\Delta H^{\ddagger}$, slope) and activation entropy ($\Delta S^{\ddagger}$, *y* intercept). (*d*) In Michaelis-Menten kinetics (derived from the chemical framework in panel *b*), the production rate depends on the catalytic rate (k_{cat}) and the Michaelis-Menten constant (K_M), which captures the effects of the forward and reverse binding rates (k_f, k_r). Increasing temperature increases K_M (*left*). At higher substrate concentrations ($[S] \gg K_M$), the reaction rate depends only on k_{cat} and its activation energy (*right*); at lower concentrations ($[S] \ll K_M$), the rate depends on k_{cat}/K_M, thereby lowering the activation energy (*left*). Colored circles represent the K_M at each temperature (*left*). (*e*) Most enzymes increase the rate of a reaction by lowering the activation enthalpy (*left*) (data from Reference 163), but rates can be enhanced through an increase in the activation entropy (*right*) (data from Reference 138).

A wealth of measurements of growth rate across temperatures has revealed a general exponential relationship consistent with the Arrhenius law of equilibrium thermodynamics, which relates chemical reaction rates to temperature through an activation energy (10, 24, 54) (**Figure 1*a***). However, underlying this seemingly simple temperature sensitivity of cellular growth is a complex network of thousands of reactions, each of which has its own temperature dependence. The details of this temperature dependence can arise from multiple thermodynamic factors (e.g., enthalpy and entropy), leading to potentially large differences in sensitivity across reactions. Moreover, the levels of each molecule can vary with temperature, as can the organism's metabolic program. Other reviews have provided excellent analyses of the heat- and cold-shock responses (70, 115), which allow for adaptation to temperature shifts outside the normal range of growth. In this review, we discuss the temperature dependence of a wide variety of central cellular processes,

aiming to identify general principles that connect temperature to growth. We start by focusing on the impact of temperature on enzymes, which form the bedrock of all biological systems and for which the Arrhenius law has a direct mechanistic framework. We then examine how growth rate changes phenomenologically across temperatures, largely focused on microbes. Next, we focus on processes within the central dogma (DNA replication, transcription, translation) and membrane synthesis, all of which can be limiting for growth, and examine how their individual temperature sensitivities could be coordinated. We discuss cellular adaptation to temperature and, in turn, how temperature may have affected evolutionary dynamics. Finally, we assess how temperature impacts complex communities of organisms, such as those that live in the soil or ocean.

ENZYME KINETICS AND THE CONNECTION TO CELLULAR GROWTH

Investigation of the impact of temperature on cellular behavior has a long history, rooted in the study of chemical reactions and the formation of the field of thermodynamics in the nineteenth century (8, 108). In classical chemical kinetics, the rate of a chemical reaction at equilibrium depends on temperature according to the empirical Arrhenius equation (8) (**Figure 1*a***):

$$k = Ae^{-\frac{E_a}{k_B T}}. \quad 1.$$

Equation 1 describes the intuitive result that an increase in temperature (T) causes an increase in reaction rate (k) because the relative cost of the activation energy (E_a) is reduced compared with the thermal energy $k_B T$. A is a constant that sets the maximum reaction rate. As E_a is typically much larger than $k_B T$, small changes in temperature can produce large changes in k; for example, the rate of a reaction with a moderate E_a of 25 $k_B T$ would increase twofold upon a 10°C temperature increase. Equation 1 typically holds only over a limited range of temperatures that is reaction dependent; for a review focused on enzyme kinetics, including non-Arrhenius behavior, the reader is referred to Reference 7.

According to transition-state theory, the activation energy reflects the change in enthalpy (total heat content) required to reach a transition state, which for enzymes describes the substrate-bound enzyme (39) (**Figure 1*b***). Thus, thermodynamic properties of the activated state can be inferred by varying the temperature of a reaction and measuring the change in reaction rate; the slope relates to the activation enthalpy $\Delta H^{\ddagger}$, and the intercept relates to the activation entropy $\Delta S^{\ddagger}$ (difference between initial and transition states) (39), as described by the Eyring equation (**Figure 1*c***):

$$k \propto e^{\frac{\Delta S^{\ddagger}}{k_B}} e^{-\frac{\Delta H^{\ddagger}}{k_B T}}. \quad 2.$$

The activation energy in the Arrhenius equation is equal to the activation enthalpy offset by the thermal energy (which only contributes approximately 0.6 kcal/mol): $E_a = \Delta H^{\ddagger} + k_B T$; thus, reported values of E_a and $\Delta H^{\ddagger}$ are approximately interchangeable.

In classical enzyme kinetic theory, the Michaelis-Menten equation is derived from a reversible transition state of the substrate-bound enzyme (141). Since the reaction is reversible, the forward and reverse rates are both temperature dependent, and so K_M depends on temperature (**Figure 1*d***), typically in an increasing fashion (141). Thus, since enzyme-catalyzed synthesis is dictated by k_{cat}/K_M rather than k_{cat} at subsaturating substrate concentrations, the activation energy of reactions in this regime is predicted to be lower than at saturation (**Figure 1*d***), consistent with experimental findings (37). While in vitro experiments typically provide substrates at saturating concentrations (100), cells regularly confront low-nutrient conditions in their natural environments (123), during which temperature-dependent effects may be reduced.

Enzymes have evolved to lower the activation energy of reactions with low uncatalyzed rates (37, 163), thereby increasing reaction rates at biological temperatures (**Figure 1*e***). For example, uncatalyzed hydrolysis of glycosides occurs very slowly (approximately 10^{-6} s^{-1}) but increases to approximately 1 s^{-1} in the presence of alpha-glucosidase through a decrease in $\Delta H^{\ddagger}$ from 30 to 11 kcal/mol ($k_B T = 0.6$ kcal/mol at 25°C) (163). A survey of enzyme catalysis across bacterial species whose normal growth temperatures span from 4°C to 100°C showed that enzymes have similar activation energies (approximately 8–18 kcal/mol) independent of growth temperature (37, 104). The empirical minimum activation energy of approximately 8 kcal/mol (37, 163) across nature may indicate a limit to the catalytic capacity of enzymes.

However, enzymes have thermal limits: Catalytic rates increase until an optimal temperature is reached, above which the rate falls rapidly due to enzyme denaturation (141). Thus, a challenge for all cellular systems is enzyme stability: The time required for protein maturation limits the rate of enzyme production, while destabilization of active enzymes increases at higher temperatures (130). At high temperatures, cells respond to increased protein unfolding using molecular chaperones that are induced as part of the well-characterized heat-shock response (115), but chaperone production diverts translational capacity from other processes. These obstacles are thought to limit the maximum growth rate across temperatures (20).

FACTORS THAT INFLUENCE ACTIVATION ENERGY

The action of *Escherichia coli* dehydrogenases on a variety of substrates exhibited a common activation energy of approximately 20 kcal/mol despite an approximately 100-fold range in reaction rates (51), suggesting that some enzyme-catalyzed chemistries may have a conserved temperature dependence. Nonetheless, environmental factors can alter enzyme activation energy. For example, increased salt concentration dramatically increased both reaction rates and the activation energy of purified ATPase (52). Activation energies may also depend on subcellular localization, as membrane-bound ATPase and ribosomes from rat liver exhibited higher rates of ATP and protein production, respectively, as well as higher activation energies, compared with freely diffusing molecules (111, 150). Thus, the temperature dependence of each cellular process may be context specific and depend on a host of environmental variables that remain to be elucidated.

THE IMPACT OF TEMPERATURE ON GROWTH RATE ACROSS ORGANISMS

The most well-studied organism, *E. coli*, is commonly grown in the laboratory at 37°C, a temperature chosen based on *E. coli* colonization of the human body. However, *E. coli* achieves its maximum growth rate above 37°C (approximately 40°C for laboratory strains) and can tolerate a broad range of temperatures (4–45°C). Interestingly, the temperature dependence of growth rate [defined as the rate of change in log(optical density)] in *E. coli* follows an Arrhenius law between 20 and 37°C (**Figure 2*a***), mimicking a single rate-limiting reaction with an activation energy (approximately 13 kcal/mol) similar to the free energy from ATP hydrolysis (54, 108) despite growth being the result of thousands of coupled reactions (20, 56, 114). The range of temperatures over which log(growth rate) versus $1/T$ is linear has been termed the Arrhenius range (20, 54) (**Figure 2*a***). *E. coli* exhibited similar activation energies (13–15 kcal/mol) during growth in a variety of media (21, 54, 99), suggesting that activation energy may be independent of the specific metabolic pathways used for growth. Additionally, the maximum yield of *E. coli* cultures varied significantly across carbon sources but was constant between 22°C and 37°C (21), indicating that metabolic efficiency is preserved within the Arrhenius range.

How conserved is the temperature dependence of *E. coli* growth? Bacterial species with a wide range of optimal growth temperatures (14–71°C) grown in the same medium displayed activation

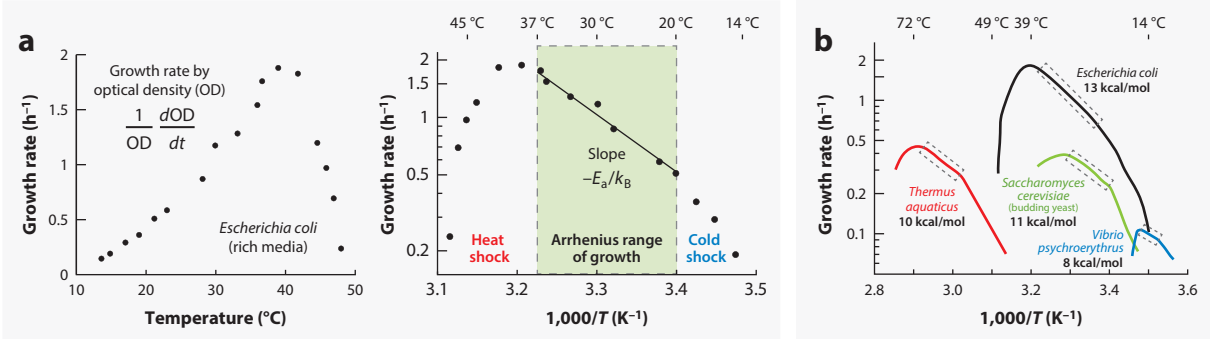

Figure 2

Cellular growth rates obey species-specific Arrhenius laws. (*a*) Growth rates of *Escherichia coli* in rich medium were measured at various temperatures (*left*). An Arrhenius plot [log(growth rate) versus 1/*T*] reveals a range of temperatures (20–37°C) over which the data are approximately linear, a so-called Arrhenius range (*right*). Temperatures above and below the Arrhenius range produce a heat- and cold-shock response, respectively. Data from Reference 54. (*b*) Bacterial and eukaryotic species possess Arrhenius ranges (*dotted boxes*) with similar activation energies, despite a wide range of growth temperatures and growth rates (*E. coli*, data from Reference 54; *Thermus aquaticus*, data from Reference 99; *Saccharomyces cerevisiae*, data from Reference 156; *Vibrio pyschroerythrus*, data from Reference 99).

energies ranging from 6 to 33 kcal/mol, with most falling between 8 and 15 kcal/mol (99). Interestingly, *Vibrio marinus* had the highest activation energy (33 kcal/mol) and lowest optimal temperature (14°C) (99), suggesting a possible correlation between temperature sensitivity and growth at low temperatures. However, in soil bacteria, a positive correlation between activation energy and minimum growth temperature has been observed (75). Across several thermophiles with similar optimal growth temperatures (60–65°C), a negative correlation exists between E_a (8–39 kcal/mol) and growth rate (0.4–2 h^{-1}) at the optimal temperature (27, 55, 106), suggesting a trade-off between temperature sensitivity and maximum growth rate.

Nonbacterial species, ranging from archaea to mammalian cell types, also exhibit species-specific Arrhenius laws (**Figure 2*b***). A study of 14 archaeal species from the family Halobacteriaceae revealed relatively high and narrowly distributed optimal growth temperatures (43–50°C) with low activation energies between 5 and 10 kcal/mol (117), suggesting phylogenetic conservation of E_a. Mammalian cells have much narrower Arrhenius ranges and higher activation energies than do bacteria and archaea: HeLa cells grown in liquid suspension have a narrow Arrhenius range (33–38°C) and $E_a \approx 31$ kcal/mol (113), and leukemic mouse cells have an E_a of approximately 32 kcal/mol between 31°C and 37°C (160). By contrast, yeasts appear to be more similar to bacteria: The starch-converting yeast *Lipomyces kononenkoae* has a relatively wide Arrhenius range (25–33°C) and $E_a \approx 12$ kcal/mol (143). While these observations motivate speculation about the relationships among phylogeny, optimal growth temperature, growth rate, and activation energy, uncovering the general rules will require a more comprehensive and quantitative interrogation of the temperature dependence of growth across taxonomic groups.

THE IMPACT OF TEMPERATURE ON CENTRAL DOGMA PROCESSES: DNA REPLICATION, TRANSCRIPTION, AND TRANSLATION

Growth rate reflects the speed of cellular duplication, requiring that all steps of the central dogma (DNA replication, transcription, and translation) occur at similar rates to each other and to volume expansion to maintain homeostasis. Thus, when growth rate increases due to a temperature increase, the rates of polymerases involved in central dogma processes likely increase

in tandem, suggesting that either their activation energies are the same or additional regulation is required. In the sections below, we present an overview of the numerous studies focused on the temperature dependence of the core polymerases [DNA polymerase (DNAP), RNA polymerase (RNAP), the ribosome] in an effort to synthesize a framework of how central processes are coordinated across temperatures.

DNA Replication

Growth rate is often varied experimentally via nutrient limitation such that DNA replication, biomass production, and cellular expansion are all ultimately limited by the same pool of precursor material. If, instead, growth rate is modulated through changes in temperature, then it is reasonable to assume that, unless DNAP and the cellular growth machinery have the same temperature sensitivity, DNA replication and growth must be coordinated to ensure proper proliferation at each temperature.

Radiolabeling of DNA in dividing *E. coli* cells to study the interplay between growth and DNA replication revealed that the time required for DNA replication was double the time between division and initiation of replication, regardless of nutrient condition or temperature (109), indicating that DNA replication rate is dependent on both nutrient availability and temperature. Nonetheless, DNA concentration is constant across nutrient conditions and temperature in *E. coli* (21), *Salmonella* Typhimurium (131), and budding yeast (156), demonstrating highly conserved coordination between DNA replication and growth.

In vitro, purified *E. coli* DNAP I incorporates radiolabeled nucleotides at a speed that depends on temperature according to an Arrhenius law with an activation energy of 17 kcal/mol over a broad range of temperatures (4–40°C) (92) (**Figure 3*a***). This activation energy is consistent with early studies of radiation damage in *E. coli*, in which gamma irradiation initiates DNA degradation at a temperature-dependent speed with an E_a of 17 kcal/mol (19); this degradation is accomplished in coordination with DNAP (151). In vitro measurements of the speed of the Klenow fragment (the catalytic component of *E. coli* DNAP I) also showed Arrhenius behavior with an $E_a \approx$ 24 kcal/mol (13), suggesting that the full DNAP is less temperature sensitive than the Klenow fragment. Since the activation energy of *E. coli* DNAP I (17 kcal/mol) is slightly higher than that of growth (13–15 kcal/mol) (21, 54, 99), maintenance of DNA concentration across temperatures may depend on additional factors, including the entire suite of DNAPs (I–V) (44), whose temperature dependence is not yet known.

DNAPs from other organisms also exhibit Arrhenius behavior. DNA replication speed in cultured hamster fibroblasts and HeLa cells had an $E_a \approx$ 22 kcal/mol between 31°C and 39°C (126), and in kidney cells from *Xenopus laevis* grown between 18°C and 28°C, the activation energy of replication speed was 18 kcal/mol (3), similar to *E. coli* DNAP I. However, in extremophiles, a large range of activation energies has been observed. In vitro, the well-known Taq polymerase (DNAP isolated from *Thermus aquaticus*) used for PCR exhibited an E_a of approximately 22 kcal/mol (73), and the Klentaq catalytic fragment of Taq displayed a similar $E_a \approx$ 24 kcal/mol between 25°C and 60°C (13). Isolated DNAP from the archaeal hyperthermophile *Thermococcus litoralis* had an activation energy of 22 kcal/mol between 30°C and 75°C (69). By contrast, a catalytic fragment of DNAP from the thermophilic bacterium *Geobacillus anatolicus* had an $E_a \approx$ 13 kcal/mol in vitro between 22°C and 50°C; error frequency was constant across temperatures (16). Replication speed of DNAP from the archaeal thermophile *Sulfolobus solfataricus* had an activation energy of 33 kcal/mol between 26°C and 56°C in vitro (42). Thus, the temperature dependence of DNA replication may not be conserved across bacterial species and has no obvious connection to natural growth temperatures.

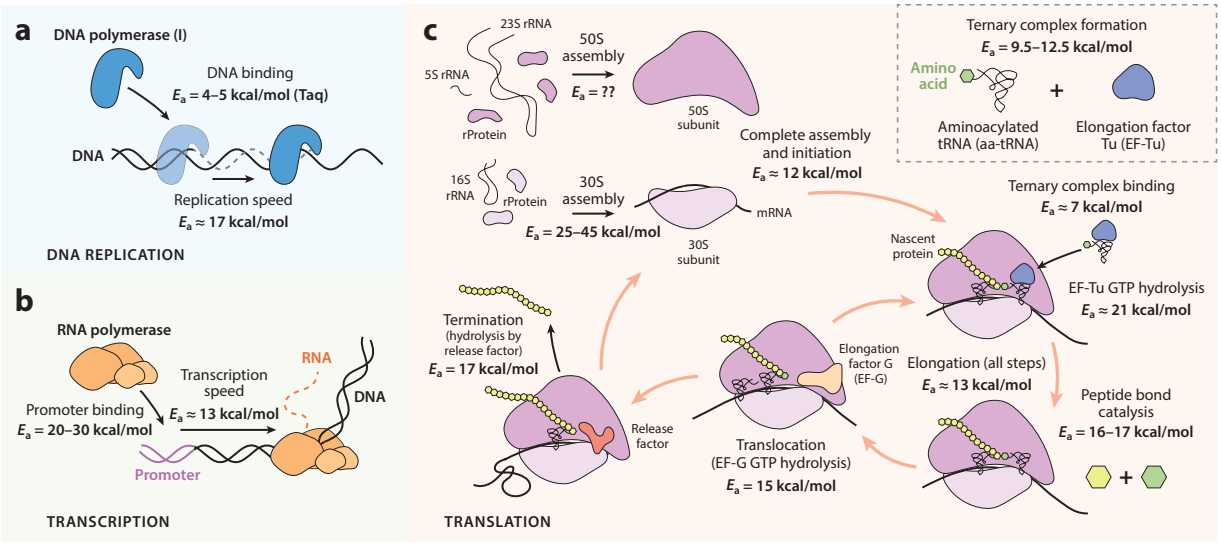

Figure 3

The effects of temperature on central dogma processes. (*a*) DNA polymerase I (*blue*) from *Escherichia coli* binds DNA templates with a low activation energy (E_a) (data from Reference 73) and synthesizes DNA at a speed that obeys an Arrhenius law ($E_a \approx 17$ kcal/mol) (data from Reference 92). (*b*) The multisubunit RNA polymerase from *E. coli* (*orange*) binds promoters with a relatively high E_a (data from References 36, 63, 121, 122, and 159) and synthesizes RNA across temperatures with an E_a that agrees with growth (approximately 13 kcal/mol) (data from Reference 1). (*c*) The bacterial ribosome (values shown for *E. coli*) is assembled from RNA and protein components to form the 30S and 50S subunits (data from Reference 147), which associate to form the full 70S ribosome during translation (data from Reference 2). Each stage of translation is temperature dependent, and catalytic steps possess a narrow range of activation energies (E_a = 15–21 kcal/mol) (data from References 40, 62, 65, 72, 74, 118, 133, and 138). Abbreviations: mRNA, messenger RNA; rRNA, ribosomal RNA; tRNA, transfer RNA.

While DNAP speed is likely rate limiting for DNA replication under saturating substrate concentrations, the complex interplay between DNA accessibility and polymerase binding must be thermodynamically compatible to ensure proper binding and polymerase initiation (**Figure 3*a***). For example, force measurements of tethered DNA templates showed that the persistence length (L_p) of DNA decreases with increasing temperature (35), as is expected based on statistical mechanics (108). L_p increased with G+C content and decreased due to binding and compaction by the *E. coli* histone-like HU protein, regardless of temperature (35). Interestingly, HU binding was strong enough to overcome the temperature dependence of L_p, indicating that the effects of temperature changes can be alleviated by protein binding.

Fluorescence anisotropy measurements showed that the Klentaq fragment and full Taq optimally bind DNA at approximately 50°C (28), whereas the Klenow fragment binds optimally at 25°C (29); the exact temperature dependence of DNA binding by DNAP remains unclear. Some studies have measured a highly nonlinear (i.e., non-Arrhenius) temperature dependence of both Klenow and Klentaq polymerases (28, 29, 164), but recent measurements of the kinetics of Taq binding to DNA substrates showed Arrhenius behavior across a large range of temperatures (5–55°C) with a very low E_a of 4–5 kcal/mol (73) (**Figure 3*a***). This discrepancy may be due to experimental differences, given the large differences in measured dissociation constants: K_d of approximately 6 nM in Reference 29 and approximately 5 pM in Reference 73. Thus, further work is needed to fully understand the effects of temperature on DNAP–DNA binding.

Transcription

To coordinate increased metabolic flux and growth rates at higher temperatures, cells must alter their gene expression program to account for temperature-dependent increases in messenger RNA (mRNA) production by RNAP, in addition to changes to binding and unbinding rates of RNAP and transcription factors at promoter regions (**Figure 3*b***). RNAP concentration in *E. coli* is constant across normal growth temperatures (54), representing approximately 1% of the total proteome between 25°C and 42°C in minimal glucose medium (125). In both minimal and rich media, the concentration of total RNA in *E. coli* depends on nutrient quality but not temperature (21, 125).

Since total RNA and RNAP concentrations are both constant across temperatures, the rate of RNA synthesis by RNAP must be coordinated with growth rate. Indeed, the incorporation rate of radiolabeled ribonucleotides in *E. coli* cells at 29°C and 37.5°C exhibits an E_a of 11 kcal/mol in rich media (87), similar to the E_a of growth rate (13–15 kcal/mol) (21, 54). The RNA synthesis rate per DNA molecule across temperatures in *E. coli* computed from RNA and DNA content produced the same E_a of 11 kcal/mol (21). Pulse-chase experiments with radiolabeled uridine showed an increase in chain elongation rate from 32 to 118 nt/s when temperature was increased from 20.5°C to 42°C, consistent with an E_a of approximately 11 kcal/mol (125). Single-molecule experiments confirmed the temperature dependence of *E. coli* RNAP speed, measuring an activation energy of 13 kcal/mol while finding that pausing and unpausing rates are approximately temperature invariant (1) (**Figure 3*b***).

While RNAP speed is limiting for RNA synthesis after transcription initiation (intracellular NTP concentration is approximately 1 mM; RNAP saturates at approximately 100 μM) (14, 142), the kinetics of DNA binding, promoter recognition, and transcription initiation by RNAP may have temperature dependences that impact overall gene regulation separate from thermal effects on catalytic speed. In vitro, *E. coli* RNAP bound to the λ phage pR promoter with an association constant that increased between 25°C and 37°C and with an activation energy of 20 kcal/mol, while the dissociation constant had an inverse relationship with temperature ($E_a \approx -9$ kcal/mol) (121, 122), indicating highly favorable binding. *E. coli* RNAP bound to the T7 phage A1 promoter with an association constant E_a of approximately 16 kcal/mol (63), and association of *E. coli* RNAP to the *tetR* promoter in vitro had an activation energy of 31 kcal/mol (36). Furthermore, in vitro studies examining the impact of specific promoters on transcription rates (including both association and polymerization) revealed generally high, promoter-dependent activation energies compared with the E_a of growth rate (13–15 kcal/mol). *E. coli* RNAP transcription rates from viral T4 DNA had an activation energy of 23 kcal/mol (159), and transcription from λ phage promoter regions resulted in activation energies of 23 and 25 kcal/mol (91). Transcription of a synthetic DNA template depended more weakly on temperature than did viral DNA templates ($E_a \approx 8$ kcal/mol) (91), suggesting that promoters may have evolved to have high activation energies. These results suggest that specific promoters can have dramatically different temperature-dependent transcriptional behavior (**Figure 3*b***).

Like growth rate, the Arrhenius behavior of RNAP appears to be conserved, with species-specific activation energies. Purified RNAP from the Antarctic-dwelling bacterium *Pseudomonas syringae* had synthesis speeds with an E_a of 35 kcal/mol between 0°C and 16°C (153), substantially higher than the E_a of *E. coli* RNAP (21). In budding yeast, RNAP II (responsible for mRNA synthesis) transcription in vivo had an E_a of 8.5 kcal/mol between 23°C and 37°C (96); in contrast to *E. coli*, the cellular concentration of RNAP II decreased slightly with temperature (96), suggesting complex regulation that ensures proper RNA levels. Due to the small number of existing studies, it is unclear whether the activation energies of growth rate and RNAP speed are correlated.

RNAPs isolated from viruses exhibit Arrhenius behavior with high temperature sensitivity. In vitro, viral RNAP from avian influenza had a large E_a of 27 kcal/mol between 26°C and 37°C, with RNA synthesis rates falling sharply above 39°C (132), suggesting that viral RNAP may have evolved to operate optimally at host body temperatures. Transcription of very short DNA fragments (5 base pairs) by T7 viral RNAP was used to estimate the rate of initiation, leading to the finding that single-stranded and double-stranded templates have similar activation energies (25 and 26 kcal/mol, respectively), despite single-stranded DNA having higher initiation rates (90, 152). Thus, transcription initiation by T7 RNAP is strongly temperature dependent, likely owing to a large enthalpic change that occurs after rapid DNA melting.

Translation

Quantification of the chemical composition of cells has established a bacterial growth law in which growth rate across nutrient conditions correlates linearly with the cellular concentration of ribosomes (131, 134, 145); this law appears to be conserved across prokaryotes and even eukaryotes such as budding yeast (158). These studies suggest that ribosome concentration varies across nutrient conditions to match the availability and synthesis capacity of free amino acids (**Figure 4*a***). However, the correlations among growth rate, ribosome concentration, and transfer RNA (tRNA) levels break down when growth rate is varied by temperature. A seminal study of the effects of temperature on *E. coli* examined the abundances of 133 proteins between 13.5°C and 46°C in rich medium; the included ribosomal proteins varied only slightly with temperature between 13.5°C and 42°C (54), suggesting that ribosome concentration is constant across the normal growth range of temperatures. Furthermore, the RNA–protein ratio (a common proxy for ribosome concentration) remained approximately constant between 21°C and 42°C in rich medium (125), and direct quantification confirmed a constant proteome fraction accounting for ribosomal proteins in *E. coli* between 30°C and 42°C (167). The fixed ribosome concentration across temperatures (**Figure 4*a***) suggests that the resulting changes in growth rate are not limited by ribosome number but instead are likely limited through a kinetic process.

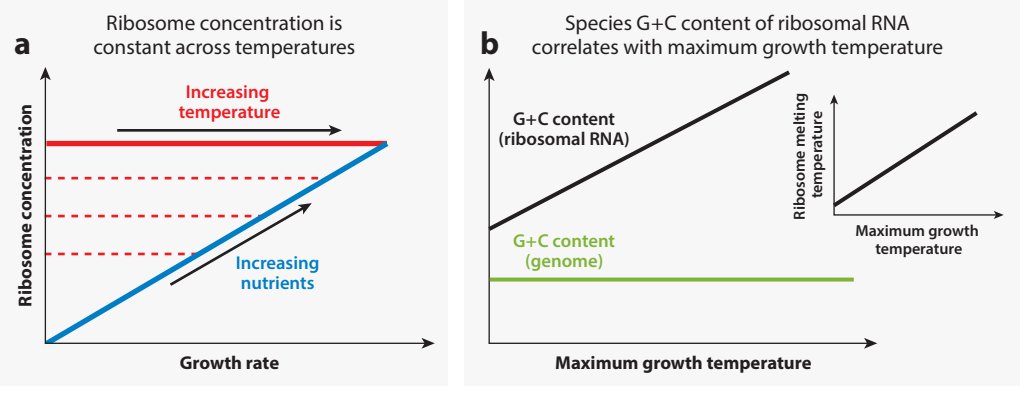

Figure 4

Ribosome concentration is constant across temperatures, and ribosome stability correlates with the maximum growth temperature. (*a*) The canonical growth law states that growth rate is linearly related to the ribosome concentration across media of varying nutrient content (*blue line*). However, ribosome concentration is constant across temperatures, despite variations in growth rate (*red line*; *dotted lines* at different nutrient conditions). (*b*) The G+C content of ribosomal RNA (*black*), but not that of the genome (*green*), correlates with the maximum growth temperature. (*Inset*) The ribosome melting temperature across species also correlates with the maximum growth temperature. Data from References 48 and 107.

THE TEMPERATURE DEPENDENCE OF RIBOSOME ASSEMBLY

An important component in translational control is ribosome assembly, which in *E. coli* requires the coordination of 54 proteins and 3 large RNAs [ribosomal RNAs (rRNAs)] (**Figure 3*c***). These components form into separate small (30S) and large (50S) subunits that mature into full (70S) ribosomes assisted by an array of enzymes (137) (**Figure 3*c***). The timescale for complete ribosome assembly is rapid compared with the doubling time, with 50S assembly occurring within minutes (136). The speed of ribosome assembly depends on growth conditions: Across media, the time for rRNA incorporation into 70S *E. coli* ribosomes was a constant fraction of the doubling time (approximately 0.05–0.06) (95). The maturation time of rRNA into 30S and 50S particles similarly scales with doubling time (79).

Dissection of the complete assembly kinetics of the *E. coli* 30S subunit in vitro between 15°C and 40°C revealed a large range of activation energies for binding of various ribosomal proteins to 16S rRNA (25–45 kcal/mol) (**Figure 3*c***). Interestingly, the binding rate constant was inversely correlated with the binding activation energy (147). According to the Eyring equation (Equation 2; **Figure 1*c***), the reaction rate is inversely correlated to the activation energy only if the activation entropy is constant, suggesting that the entropic cost of binding to rRNA is similar for all ribosomal proteins.

Measurements of the fractions of 30S, 50S, and 70S subunits in *E. coli* cell extract showed that the equilibrium association constant for fully mature ribosomes (K_a = [70S]/[30S][50S]) was as high as 10^{26} M^{-1} under certain ionic conditions, indicating a strong affinity between small and large subunits (32). Increases in temperature favor dissociation of the complex, with a very large and negative E_a of −85 kcal/mol in the association constant (32, 57). Association is Mg^{2+} dependent due to the large negative charge of rRNAs, and Mg^{2+} concentration correlated positively with activation energy (57), consistent with predictions from Michaelis-Menten kinetics (**Figure 1*d***). Thus, while subunit association decreases with temperature, affinity is remarkably high and is likely not limiting for translation.

The temperature dependence of ribosome assembly in vivo is unclear; the large discrepancy between the activation enthalpies of 30S–50S association and of ribosomal protein binding to rRNA must somehow be coordinated to produce complete subunits and fully mature ribosomes across temperatures. One study (2) examined *E. coli* ribosome assembly in cells with and without chaperones across a range of temperatures, reasoning that assisted protein folding would be necessary at high temperatures. In wild-type cells, complete incorporation of radiolabeled rRNA into mature ribosomes took approximately 15 min at 30°C and approximately 8 min at 40°C (2), indicating an assembly rate E_a of approximately 12 kcal/mol, similar to that of growth rate (54) (**Figure 3*c***). When cells lacked the chaperone DnaK, the assembly time more than doubled at both 30°C and 40°C, with increased abundances of subunit intermediates (21S, 32S, 45S) (2), suggesting a role for chaperones in late-stage ribosome assembly regardless of temperature.

THE TEMPERATURE DEPENDENCE OF TRANSLATION RATE

Once ribosome assembly is complete (1–2 min during fast growth) (79, 95) and a transcript is bound for translation, translation occurs in a sequence of initiation, elongation, and termination (77) (**Figure 3*c***). Each of these steps is enzymatically catalyzed and is therefore temperature dependent (37, 163). Since ribosome and protein concentrations are approximately constant as a function of temperature (125), the increase in protein production rate that accompanies higher growth rates at higher temperatures must be accomplished through an increase in the translation rate of the ribosome.

Measurement of the in vivo rate of protein production in *E. coli* between 10°C and 44°C was elegantly accomplished by isopropyl β-D-1-thiogalactopyranoside (IPTG) induction of β-galactosidase (β-gal), wherein the first signal of β-gal activity in cell extracts indicated the time of completed translation (40). These data showed that the translation rate increased according to an Arrhenius law from approximately 6 aa/s at 23°C to approximately 19 aa/s at 44°C (40), representing an E_a of 13 kcal/mol. Below 23°C, both growth rate and translation rate decreased dramatically, and the translation rate continued to increase at heat-shock temperatures above 37°C, while the growth rate slowed (40). Thus, the translation rate in *E. coli* obeys an Arrhenius law across a large temperature range (23°C to at least 44°C) with an E_a consistent with growth (13 kcal/mol) (40) (**Figure 3*c***).

During translation, aminoacylated tRNAs (aa-tRNAs) are delivered to the ribosome by the GTPase elongation factor Tu (EF-Tu) in what is termed the elongation ternary complex (EF-Tu, GTP, and aa-tRNA) (118) (**Figure 3*c***). In vitro measurements of ternary complex formation across temperatures found that noncognate tRNAs bind EF-Tu with affinities similar to those of cognate tRNAs. However, cognate tRNAs bound EF-Tu with a much narrower range of binding free energy (9.5–10.5 kcal/mol) and binding activation energy (9.5–12.5 kcal/mol) (74) (**Figure 3*c***). The dissociation constant of the elongation ternary complex and the *E. coli* ribosome (23 nM at 37°C) has an activation energy of approximately 7 kcal/mol (118). Other kinetic parameters for this binding were inferred to have similarly small activation energies, ranging from 2 to 10 kcal/mol (118) (**Figure 3*c***). GTP hydrolysis by EF-Tu, which arranges aa-tRNAs for reaction with the growing peptide chain, exhibited a relatively large activation energy (21 kcal/mol) and activation entropy (7 kcal/mol) (62) (**Figure 3*c***), indicating high catalysis rate and temperature sensitivity.

After the aa-tRNA is positioned by EF-Tu, the ribosome catalyzes the peptide bond between the tRNA-bound amino acid and the growing protein (**Figure 3*c***). To interrogate the thermodynamics of catalysis of peptide bond formation across temperatures, an in vitro chemical system for comparing peptide bond kinetics in solution against the reaction catalyzed by purified *E. coli* ribosomes was developed (138). Peptide bonds formed in solution had a lower activation energy than those catalyzed by ribosomes ($E_a \approx 9.7$ kcal/mol in solution versus $E_a \approx 17$ kcal/mol for those catalyzed by ribosomes) and dramatically different activation entropies ($T\Delta S^{\text{solution}} \approx -13$ kcal/mol versus $T\Delta S^{\text{ribosome}} \approx 0.7$ kcal/mol) (138) (**Figure 3*c***). Similar studies of in vitro peptide-bond catalysis by ribosomes found activation enthalpies of 16–17 kcal/mol and an activation entropy of approximately 2 kcal/mol (62, 133), in close agreement with Reference 138. Thus, unlike typical enzymes, which enhance rates through lowering the activation enthalpy (163), the ribosome performs catalysis through increasing the activation entropy, a so-called entropy trap mechanism (138) (**Figure 1*e***).

Ribosomes continue to elongate the growing protein until the stop codon is recognized, after which release factors bind to the ribosome and catalyze release of the completed protein (65, 72) (**Figure 3*c***). *E. coli* elongation factor G (EF-G), the GTPase that catalyzes translocation of the mRNA–tRNA–protein complex through the ribosome, was demonstrated in vitro to induce translocation with an E_a of approximately 15 kcal/mol (65) (**Figure 3*c***). Furthermore, kinetic measurements of purified *E. coli* components showed that release factor 2 catalyzes peptide release from the ribosome with an E_a of approximately 16.5 kcal/mol (72) (**Figure 3*c***). Thus, most catalytic steps of translation in *E. coli* fall within a narrow range of temperature sensitivities ($E_a = 15$–21 kcal/mol), slightly higher than both the inferred overall protein synthesis rate in vivo and the growth rate ($E_a \approx 13$ kcal/mol) (40, 54). These observations may indicate that the activation energy of the overall translation rate is a combination of both binding (low E_a) and catalytic (high E_a) activation energies, a result that would be predicted from the effects of binding

on enzyme kinetics (**Figure 1*e***) and the averaging of catalytic activation energies through coupled enzymatic reactions (60).

TRANSLATIONAL ADAPTATION TO TEMPERATURE

While protein synthesis capacity is likely to be generally under strong selection, whether ribosome kinetics are conserved beyond *E. coli* is mostly unknown. Purified ribosomes from the thermophile *Thermus thermophilus* exhibited an E_a of approximately 23 kcal/mol for peptide bond catalysis (119), significantly larger than that of the *E. coli* ribosome (62), along with a higher entropic cost (approximately 5 kcal/mol). Thus, the entropy-trap mechanism may be enhanced in thermophiles to balance the higher enthalpic cost at higher temperatures. Indeed, the *T. thermophilus* ribosome had a translation rate similar to that of *E. coli* (119), suggesting that ribosomes may have evolved to conserve high rates of synthesis across different temperatures.

In addition to simple kinetic effects of temperature on translation rates through Arrhenius behavior, longer-term exposure to temperature changes may alter overall temperature sensitivity in ribosomes. Studies of wheat ribosomes revealed interesting adaptations in activation energies: Purified ribosomes incubated at various temperatures for 48 h and then switched to different temperatures for assaying synthesis rates exhibited higher synthesis rates when preincubated at higher temperatures but lower activation energies (preincubation at 4°C resulted in $E_a = 22$ kcal/mol, while preincubation at 36°C resulted in $E_a = 13$ kcal/mol). Preincubation temperature did not affect the temperature at which ribosomes became denatured (55°C), indicating that translation efficiency but not denaturation is dependent on temperature history (41). Additionally, in *E. coli*, antibiotics that target the ribosome elicit cold-shock and heat-shock transcriptional responses (155), suggesting that the translational inhibition during temperature shocks is directly tied to ribosomal inhibition. These results support the notion that ribosomes vary structurally across temperatures and thus can sense their temperature environment through differences in stability (155); they also indicate the potential for history dependence in all ribosome-related thermal adaptation.

Ribosome stability is clearly important across species. Melting temperatures of ribosomes from 19 phylogenetically diverse organisms were narrowly distributed between 69°C and 79°C, despite optimal organismal growth temperatures ranging from 18°C to 73°C (107). Additionally, the G+C content of rRNA correlated with melting temperatures, even though the G+C content of the genome did not scale with either ribosome melting temperature or optimal growth temperature (107) (**Figure 4*b***). These data point to ribosomal efficiency as a driver of selection caused by temperature changes on evolutionary timescales.

TRANSCRIPTIONAL AND TRANSLATIONAL RESPONSES TO TEMPERATURE SHIFTS AND THE ROLE OF ppGpp

While individual enzymes can change their catalytic rates rapidly in response to a change in temperature (149), downstream biological processes resulting from gene regulation likely take much longer. In *E. coli*, production of the stress-signaling molecule guanosine-tetraphosphate (ppGpp), which regulates a vast array of stress responses in bacteria (86), initially increased rapidly after an increase in temperature and then gradually decreased, and steady-state levels were positively correlated with temperature (43, 85). Additionally, RNA synthesis rates underwent multiple stages of regulation upon a temperature upshift to 40°C characterized by rapid acceleration, deceleration, and then slow acceleration to the higher steady-state rate (85). Decreases in temperature induced rapid decreases in ppGpp and RNA synthesis to steady-state values, indicating that cells respond differentially to temperature increases versus decreases (85). Time-resolved

transcriptional profiling of *E. coli* exposed to temperature decreases showed that approximately 9% of all transcripts underwent at least a twofold change in expression within 10 min, with genes related to energy metabolism preferentially decreasing in expression (47). Consequently, transcriptional responses to temperature changes appear to be quick (10–20 min) (47, 85), likely owing to strong promoter binding and fast polymerization by RNAP (121, 122, 125), but the overall regulation of the temperature-dependent transcriptome requires further elucidation.

Under conditions of amino acid starvation, the bacterial stringent response is responsible for limiting the number of ribosomes, which is mediated by the production of ppGpp (86). This regulation optimizes ribosome concentration to ensure maximal growth rates across nutrient conditions (168). A study of the rates of protein synthesis after temperature upshifts found that most *E. coli* proteins are produced at transiently accelerated or decelerated rates before settling to a steady-state value within 40 minutes (76), consistent with the timescale of ppGpp regulation (85). In a cold-dwelling *Vibrio* species, ppGpp levels transiently increased after a shift from 0°C to 13°C, but not after one from 13°C to 0°C, suggesting that the stringent response to temperature upshifts may be conserved across bacteria (6).

THE ROLE OF TRANSFER RNAS IN THERMAL ADAPTATION

Since organisms encode less than the 61 tRNAs that would match all possible codons for amino acids, chemical modifications of tRNA to facilitate processes such as wobble base pairing are required for protein synthesis (26). As such, tRNAs are the most transcriptionally modified RNA type (80). While the ratio of tRNA to ribosome copy number in *E. coli* decreases slightly with increasing nutrient availability and growth rate (34), the concentration of tRNAs is constant across normal growth temperatures (125).

Similar to rRNAs (107), the thermostability of tRNAs likely plays an important role in thermal adaptation, as tRNA G+C content correlates with tRNA melting temperature across organisms (71). A strong correlation has been observed across species between the diversity of tRNAs (number of distinct types) and G+C content (128), and thermophiles and psychrophiles (optimal growth <10°C) have a mean of approximately 42 and 34 tRNA types, respectively (127), suggesting that noncanonical tRNA binding and wobble base pairing may be suboptimal at high temperatures and thus that higher tRNA diversity is required. Temperature shifts also alter the level of tRNA modifications in thermophiles (161); for example, an increase from 70°C to 100°C increased methylation and thiolation of tRNA bases in the hyperthermophile *Pyrococcus furiosus* (71). Thus, high temperature likely selects for both tRNA diversity and modification, although it is unclear how the fidelity of translation depends on the trade-off between these two factors. The temperature dependence of tRNA abundance and usage has yet to be clarified, but tRNAs likely represent important components of thermal adaptation strategies.

REGULATION AND ADAPTATION OF MEMBRANE FLUIDITY ACROSS TEMPERATURES

Cellular compartmentalization by the membrane is also subject to temperature dependence and regulation. Membrane fluidity is predicted to increase with temperature due to weaker intermolecular interactions (4) (**Figure 5*a***), although cells may be able to tune membrane composition to counteract these changes. Measurements of the lipid composition in *E. coli* revealed that, as temperature increases, the ratio of unsaturated-to-saturated fatty acids decreases substantially (threefold between 25°C and 37°C; **Figure 5*b***) (88). Since unsaturated fatty acids produce nonoptimal packing and thus increase fluidity within phospholipid bilayers owing to their kinked hydrocarbon chains (15), increased saturation with temperature would suggest

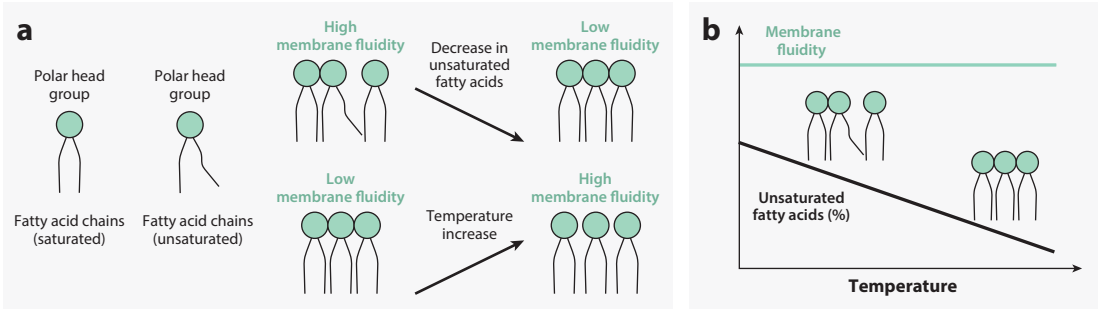

Figure 5

Homeoviscous adaptation ensures that membrane fluidity is preserved across temperatures through changes in fatty acid saturation. (*a*) The fatty acid side chains of phospholipids can be modified with varying levels of unsaturation (carbon–carbon double-bonds) that produce kinks (*left*). Without modifications to fatty acid chains, a temperature increase will increase membrane fluidity (*bottom right*). Lower levels of unsaturated (kinked) fatty acid chains produce more favorable phospholipid packing, thereby decreasing membrane fluidity (*top right*). (*b*) At higher temperatures, cells maintain membrane fluidity (*teal*) through decreasing the level of fatty acid unsaturation (*black*), counteracting the physical consequences of increased membrane fluidity at higher temperatures.

regulation that maintains membrane fluidity (**Figure 5*a***). Indeed, in *E. coli*, membrane viscosity (inverse of fluidity) was approximately constant between 15°C and 43°C (140) (**Figure 5*b***). Furthermore, isolated membranes from cells cultured at 43°C exhibited a sevenfold increase in viscosity when incubated at 15°C (140), indicating that cells adapted to high temperature have highly rigid membranes. This regulation of membrane viscosity, termed homeoviscous adaptation (140), has also been observed in yeast (15), worms (83), fish (25), and mammalian cells (5), with some regulation occurring through addition of cholesterol to rigidify membranes (5). Additionally, increases in saturated and branched fatty acid content with temperature have been observed within psychrophiles (102) and across organisms whose growth spans 5–70°C (53, 139). Taken together, these findings indicate that the ability to modify fatty acid composition across temperatures to maintain membrane fluidity is likely conserved across kingdoms.

A striking feature of the temperature dependence of membrane viscosity is that it too follows an Arrhenius law across bacterial (140), plant, and mammalian (112) membranes. In synaptic membranes, the sensitivity of membrane viscosity to temperature was nearly identical in fish and rats ($E_a \approx 13$ kcal/mol) (25), even though fish lack body temperature regulation. Despite the requirement of more rigid membranes in thermophiles to maintain proper membrane fluidity, isolated membranes still exhibited similar temperature sensitivities ($E_a \approx 11$ kcal/mol) (98). The mechanistic origins of this Arrhenius behavior are still unclear (135), although activation energies are remarkably similar to those of enzymatically catalyzed processes (1, 62, 141).

Cells may tightly regulate membrane viscosity due to a variety of processes, for example, maintenance of membrane potential. Proton import by membranes isolated from bacteria spanning optimal growth temperatures from 5°C to 95°C revealed a remarkable conservation of temperature sensitivity ($E_a = 9.5$–13 kcal/mol) and maximal rate constants (approximately 0.1 s^{-1}), and temperature-dependent sodium efflux was nearly identical across organisms and fell along a similar temperature-dependent curve ($E_a \approx 12$ kcal/mol) (154); both of these observations support the importance of membrane potential regulation. Increases in membrane fluidity led to increased cellular respiration in bacteria and mitochondria and thus allowed for increased growth rate under oxygen exposure (15), demonstrating a direct link between fluidity and physiology. Moreover, misregulation of fatty acid synthesis can have dire consequences, affecting heat tolerance (83), metabolism, and cell size regulation (15).

Interestingly, measurements of membrane viscosity have repeatedly revealed phase transitions, identified through changes to the slope of or discontinuities in Arrhenius plots (15, 112, 140). These transitions likely indicate critical temperatures at which the membrane undergoes significant rearrangement. At increasing levels of fatty acid saturation, the critical temperature increases (15, 140), probably due to increased packing that increases the heat capacity of the membrane. Alterations to phase-transition properties of the membrane can have significant functional consequences for enzyme behavior. For example, around a critical temperature of 23°C, protein synthesis rates of membrane-bound ribosomes exhibited a sharp change in slope representing a transition in E_a from 30 to 12 kcal/mol, while free ribosomes exhibited a constant E_a of approximately 25 kcal/mol (150). Various membrane-bound enzymes that exhibited critical temperatures generally showed a significant decrease (2- to 10-fold) in activation energy (166), indicating that membrane properties can significantly impact the temperature sensitivity of enzymes. Thus, the membrane (and perhaps other components of the cell envelope) can affect temperature sensitivity at the molecular and cellular scales.

ADAPTATION AND THE EFFECTS OF TEMPERATURE ON EVOLUTION

Beyond the central dogma and membrane fluidity, other cellular and ecological processes appear to depend on temperature in a manner similar to enzyme kinetics. The mass-normalized metabolic rate (based on oxygen flux) across all kingdoms has a remarkably conserved Arrhenius law, with activation energies between 6 and 11 kcal/mol (49). A similar relationship has also been observed in entire ecosystems, as measured by regional CO_2 output, with an average activation energy of approximately 9.3 kcal/mol (38). Thus, the temperature dependence of the energy requirements for life may be conserved, from individual enzymes to entire ecosystems. Despite the apparent conservation of activation energies, planetary temperature changes on evolutionary timescales have nonetheless likely constrained enzymatic function. For instance, ancient versions of the highly conserved adenylate kinase inferred from its phylogenetic tree resemble modern thermophile homologs (104) (**Figure 6*a***), consistent with the history of a cooling Earth.

Organismal fitness likely depends on the ability of each species to exploit the effects of temperature; for example, mammals may have evolved to maintain energetically costly and elevated temperatures as a means to combat fungal pathogens (17). By contrast, microorganisms are unable to regulate their intracellular temperature, and thus all biological functions are subject to variations in environmental temperature. In *E. coli*, adaptation to increased temperatures appears to have coincided with adaptation to oxygen deprivation, likely due to the anaerobic nature of the mammalian intestinal tract (146): When cells are transitioned from 37°C to 25°C, genes required for aerobic respiration are upregulated, and vice versa (146) (**Figure 6*b***).

In long-term laboratory evolution experiments, *E. coli* grown for 2,000 generations at different temperatures showed differential trade-offs in thermal adaptation, such that 32°C-evolved cells performed worse than the parent strain at 42°C, while those evolved at 42°C saw no fitness decrease at 32°C (12) (**Figure 6*c***). Interestingly, cultures alternated between 32°C and 42°C saw no fitness defect against either the ancestor or a 32°C-evolved strain at 32°C, while they exhibited a significant fitness advantage against the ancestor at 42°C (12) (**Figure 6*c***), indicating that it is possible to improve fitness over a range of temperatures simultaneously. In a follow-up study, *E. coli* was grown at 20°C, 32°C, 37°C, and 42°C for 2,000 generations, and genomic sequencing revealed beneficial mutations specific to each temperature, including loss-of-function mutations and mutations in essential genes (31). Interestingly, extended evolution of the ancestor at 37°C for 20,000 generations eventually led to many of the same mutations that benefited each temperature-evolved

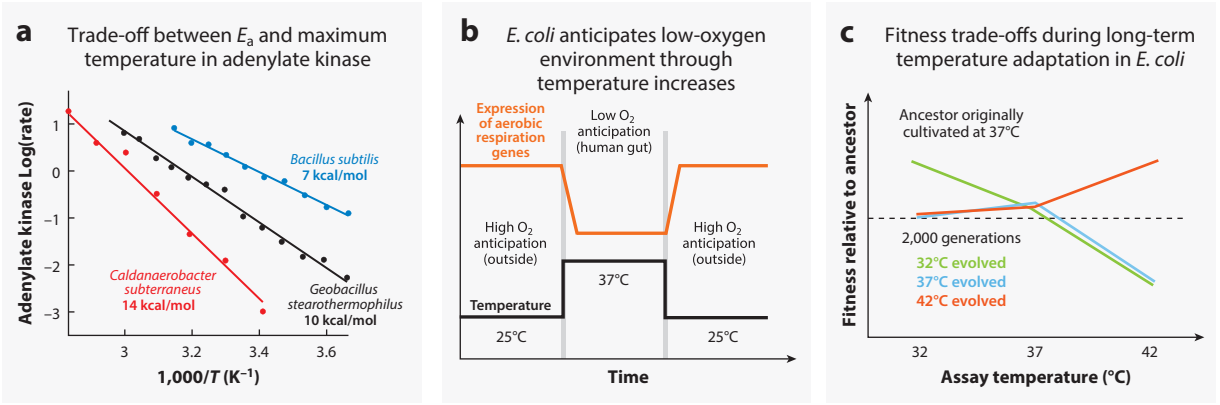

Figure 6

Thermal adaptation occurs across evolution and short-term perturbations. (*a*) The highly conserved adenylate kinase, a critical metabolic enzyme, evolved across temperatures to preserve high rates of catalysis through alterations in activation energy (higher temperature ≈ higher E_a). Data from Reference 104. (*b*) Increases in temperature from 25°C to 37°C (human body temperature) induced rapid decreases in expression of aerobic respiration genes in *Escherichia coli*, indicating convergent adaptation between exposure to increased temperature and low oxygen (reflective of the human gastrointestinal tract). Data from Reference 146. (*c*) Long-term laboratory evolution (2,000 generations) of *E. coli* to various temperatures produced optimal temperature adaptation. Cultures not evolved for high-temperature growth (42°C) suffered significant fitness defects at the higher temperature. Data from Reference 12.

strain (31), indicating that mutations can be beneficial at multiple temperatures, but temperatures other than 37°C may select for these mutations at higher frequency. In a similar study, >100 cultures of *E. coli* were independently evolved for 2,000 generations at 42.2°C; each culture increased fitness relative to the ancestor at the higher temperature with a distinct set of mutations. These mutations occurred predominantly in the RNAP complex (148), highlighting the importance of transcription in temperature adaptation. The evolved strains also shifted their permissible temperature range for growth, such that they performed worse at temperatures <20°C but better at temperatures >42°C (120).

At more extreme temperatures, dramatic trade-offs emerge between growth at normal and at high temperatures. *E. coli* evolved over the course of two years with stepwise gradual increases from 42°C to 48.5°C exhibited high and constant induction of molecular chaperones and the heat-sensitive lysine–tRNA synthetase *lysU* and suffered significant fitness defects against the ancestor at 37°C (124). Thus, adaptation to altered temperature depends on both the duration and the range of growth temperatures and is achieved through highly diverse mutational pathways, affecting a host of functional outcomes in both metabolism and global transcriptional regulation.

While individual mutations can modify the function and production of proteins to optimize growth at a given temperature, detailed analyses of how diverse organisms have evolved to thrive at temperatures spanning <0°C to >100°C paint a complex picture of thermostability requirements for DNA, RNA, and proteins (103). The traditional understanding is that protein stability is the major contributing factor for growth at high temperatures (33); thermophiles have higher protein melting temperatures (129), as well as overall higher net protein charge, than do other organisms, which is thought to counteract protein aggregation under high temperature (66). DNA composition may also play a role in thermal adaptation, although G+C content does not increase with optimal growth temperature despite the increased binding energy of G–C bonds versus A–T bonds (48, 58, 107). However, the G+C content of rRNA is correlated with optimal growth temperature (48, 107), suggesting that ribosome function is a limiting thermostability requirement

for growth at higher temperatures (**Figure 4*b***). DNA stability may still play an important role in thermal adaptation, as dinucleotide composition, which impacts DNA compaction, correlates well with optimal growth temperature (66, 103). Therefore, physical constraints on the function of central processes like translation and transcription at high temperatures may select for genomic mutations that increase stability in all biopolymers.

ECOLOGICAL IMPACTS OF TEMPERATURE VARIATION

Since every species within an ecosystem has its own profile of temperature sensitivity and adaptation, temporal fluctuations and spatial heterogeneity in temperature inevitably affect the behavior of communities. Soil bacteria in isolation possess distinct ranges of normal growth temperatures and activation energies (75, 99), suggesting the potential for temperature dependence of microbial community composition. Nonetheless, soil samples grown in media that promote either bacterial or fungal growth revealed that maximal growth rates of each occurred at 30°C, with similar activation energies from 4°C to 30°C ($E_a = 15$ kcal/mol for bacteria and 13 kcal/mol for fungi) (11), suggesting that temperature adaptation of soil communities as a whole may be approximately independent of kingdom. Samples from the same soil source were grown in parallel for one month at temperatures spanning 5°C to 50°C; after this propagation, samples grown above 30°C (but not those grown below that temperature) exhibited an increase in optimal growth temperature (11), suggesting that selection is more rapid at higher temperature. Communities of bacteria and fungi derived from agricultural and humus soil also exhibited optimal growth temperatures of approximately 30°C in vitro, but with relatively low activation energies ($E_a \approx 5$ kcal/mol) (110). By contrast, experiments in situ revealed dramatic temperature sensitivity, with a sixfold increase in microbial respiration in high-elevation alpine forest soil during the transition from winter to spring as temperature and moisture increase (101). These results suggest that soil communities may have a common optimal growth temperature, but their temperature sensitivity likely depends on the soil source (e.g., due to differences in constituent microbes).

Exposure of permafrost and active-layer soil samples to various temperatures (5°C to 40°C) for one month resulted in significant compositional changes only at the highest temperatures (81), suggesting that community composition is resilient to relatively short-term temperature perturbations. Incubation of Antarctic soil samples at temperatures above freezing (15°C) for 6 months dramatically increased nitrogen fixation (**Figure 7*a***), and subjecting samples to freeze–thaw cycles between −15°C and 10°C to simulate seasonal variation primarily affected fungal rather than bacterial composition (165). A 90-s heat shock (using a microwave) of soil-derived communities caused both immediate and gradual species loss, while 6 h of exposure to −80°C did not perturb community structure (64). It remains unknown whether elevated temperatures are generally deleterious to community composition; temperature-dependent changes to community composition may depend on phylogeny and the magnitude and duration of temperature change.

Long-term (multiyear) studies of temperature impacts on microbial communities have shown that small changes in temperature can produce large-scale metabolic and compositional changes. Metagenomic sequencing of soil samples exposed to mild heating (+2°C) for 10 years revealed that Actinobacteria preferentially grew in the warm soil, whereas Proteobacteria proliferated in unheated samples, and approximately 60% of all taxa exhibited significant differences in abundance (82). Additionally, heating caused an increase in overall G+C content, and heated samples exhibited an enrichment of genes involved in carbon utilization, respiration, and sporulation (82).

Studies from the Harvard Forest site evaluated the effects of long-term (>25 years) warming on soil biology (30, 45, 93, 94) by using buried heating cables to maintain a 5°C increase above ambient temperature in experimental soil plots (94). Soil respiration, as measured by CO_2 flux,

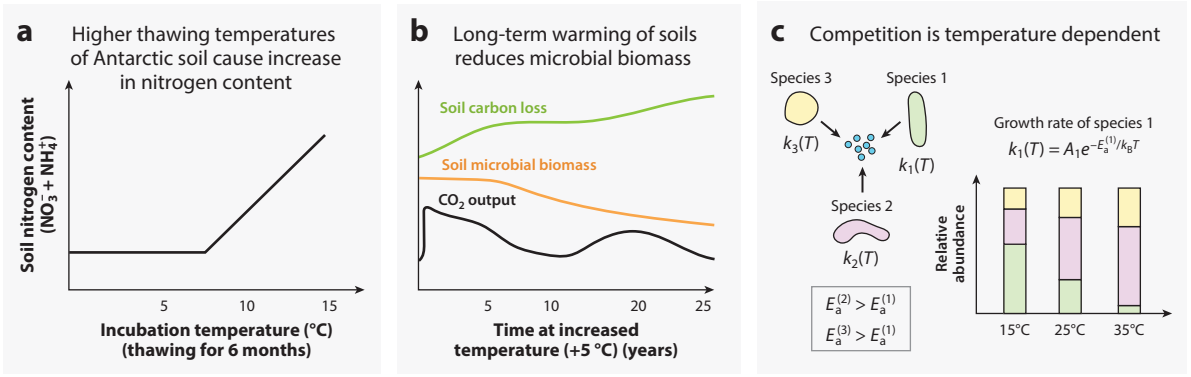

Figure 7

Microbial community behavior and composition are affected by temperature. (*a*) Antarctic soil samples thawed for 6 months at various temperatures generated a large increase in nitrogen fixation at 15°C, indicating an increase in metabolic activity. Data from Reference 165. (*b*) Long-term soil warming (+5°C above ambient) at the Harvard Forest site produced fluctuations in microbial respiration (CO_2 output, *black*), a decrease in microbial biomass (*orange*), and a net loss in soil carbon (*green*). Data from References 45 and 93. (*c*) In consumer-resource models, species competition for nutrients (*blue circles*) shapes community composition. Since species growth rate (k) and nutrient utilization are temperature dependent, increases in temperature likely select for species that possess higher activation energies (E_a) of growth.

increased significantly in the first year of heating compared to control soils; this increase was attributed to rapid utilization of simple carbon sources but eventually decreased after 10 years (94) (**Figure 7*b***). While soil microbial biomass was approximately constant throughout the first 10 years, over the following 15 years, microbial biomass decreased significantly (approximately 40%), and soil respiration accelerated (30, 45, 93) (**Figure 7*b***). Fungi experienced larger relative biomass losses than did bacteria; long-term temperature increases promoted higher bacterial diversity, particularly through increases in Acidobacteria (30). Heating also caused a decrease in the overall temperature dependence of respiration (93), suggesting that heating selects for lower activation energies at the community level (104). Importantly, through 25 years of study, heated soils generated significant carbon loss (93); it remains unclear whether ecosystems have feedback mechanisms to recover from this loss over longer timescales. Collectively, these studies demonstrate that long-term heating can reshape microbial composition in soils through increased carbon and nitrogen utilization.

DISCUSSION

A remarkable collective conclusion that emerges from the extensive studies of temperature dependence is that many biological processes, including protein binding (**Figures 1*d*** and **3**), central dogma processes (**Figure 3**), membrane fluidity (**Figure 5**), and metabolism (**Figure 6*a***), follow an Arrhenius law with activation energies that fall in a narrow range (10–20 kcal/mol). This convergence suggests that the enzyme kinetics underlying biology also dictate the emergent temperature dependence of most aspects of growth. An interesting case in point is the various kinetic steps of translation, which all have a roughly similar temperature dependence (9–21 kcal/mol) in *E. coli*, including ternary complex formation, tRNA binding, and peptide elongation (74, 118, 138) (**Figure 3*c***). This similarity may suggest an evolutionary convergence of the combined reactions to ensure stable protein synthesis across temperatures. The major polymerases of the central dogma (DNAP, RNAP, and the ribosome) in *E. coli* have a narrow range of activation energies that coincides with that of the overall growth rate (E_a = 13–15 kcal/mol). Do other enzymes from

E. coli fall within this range as well? An analysis of activation energies from the limited number of studies of enzyme kinetics demonstrated that those involved in diffusion and transport processes have lower activation energies than those involved in catabolism (116), suggesting that growth may be more limited by transport at higher temperatures. Some studies have hypothesized that the activation energy of growth represents a single rate-limiting enzymatic reaction (24), but there is no evidence to date to support this hypothesis. Other models for growth suggest that the activation energy of growth arises as an average response of all contributing reactions (56, 60). Future studies could address these models by measuring growth dynamics after temperature shifts or by targeting important pathways through chemical or genetic perturbations (67).

To what extent is cellular growth optimized across temperatures? Under varying nutrient conditions, ribosome concentration is tightly controlled to optimize protein synthesis (134, 168), but it is unclear how optimization occurs across temperatures, since ribosome concentration remains constant (54, 125, 167). Some evidence suggests that the activation energy of growth is conserved across nutrient conditions in *E. coli* (21, 54), but more detailed investigations are necessary to determine the generality of this conclusion and its mechanistic origins and implications. A large proportion of genes are differentially regulated across temperatures (47, 54, 76), but the genes responsible for temperature responses are virtually unknown, demonstrating the need for future systems-wide studies using proteomic and transcriptomic approaches (78).

A large fraction of studies of temperature dependence have focused on laboratory strains of *E. coli*; the effects of temperature on natural isolates are largely unknown. Given that temperature plays a vital role in *E. coli*'s ability to respond to oxygen availability (146), certain strains may exhibit environment- and host-specific adaptations. Moreover, detailed studies on the effects of natural variations in temperature are rare; thus, we do not yet understand how the timescales of temperature fluctuations influence responses. Laboratory long-term evolution experiments of *E. coli* have demonstrated fitness gains that are temperature specific (12), suggesting selection for increased growth rate at the target temperature, perhaps through modifying the activation energy of growth. Future studies that dissect if and how cells alter activation energy would elucidate the role of activation energy in growth and adaptation and perhaps reveal the genetic basis for such alterations.

Intracellular spatial heterogeneity in temperature may also impact which processes are more temperature sensitive, but given the complications of developing efficient thermal probes (105), few studies have been able to measure intracellular temperature. For example, temperature-dependent measurements of fluorescent proteins are particularly difficult, since maturation, denaturation, and quantum efficiency (not to mention expression dynamics) all change as a function of temperature (9). Recent measurements using thermosensitive dyes surprisingly revealed that mitochondria are maintained at approximately 50°C (22), suggesting that there are different thermostability requirements across metabolic processes.

Given the role of the environment in shaping temperature sensitivity, it is natural to speculate that activation energy is coupled to other growth behaviors. Indeed, a survey of soil bacteria revealed that activation energy is correlated with minimal growth temperature (75), and activation energy is correlated with maximal binding rate across proteins involved in 30S ribosome assembly (147). These observations suggest that species or proteins that optimally grow or bind, respectively, at higher temperatures perform comparatively worse at lower temperatures, likely reflecting trade-offs of performance optimization at high temperature that necessarily involve increases in enthalpy and entropy. While some studies have suggested the importance of protein stability in shaping temperature-dependent growth (20, 33), ribosomal and membrane stability requirements suggest other forms of adaptation (107, 139), indicating that more work is needed to understand

how distinct activation energies and maximal growth rates may arise in other organisms and how they are coupled (23).

The limited studies carried out to date on microbial communities have shown temperature-dependent composition and behavior (30, 75, 81, 82, 144) (**Figure 7**), but the mechanisms that account for these changes are mostly unknown. For example, the interactions among temperature, metabolism, and nutrient competition likely play substantial roles. Consumer-resource models have demonstrated the ability to explain species coexistence through resource competition (89), but how temperature variations affect these interactions has yet to be explored in detail (**Figure 7*c***). The use of in vitro–assembled communities should help to address these questions (6a, 50, 157). Understanding how temperature changes disrupt microbial communities will be critical to mitigating current and future effects of global warming, as exemplified by the collapse of certain ecosystems like coral reefs due to small temperature increases (46). In addition, long-term shifts toward increased temperatures can have deleterious consequences for human health, as they may select for bacterial and fungal pathogens (68), as well as antibiotic-resistant strains of bacteria (84).

DISCLOSURE STATEMENT

The authors are not aware of any affiliations, memberships, funding, or financial holdings that might be perceived as affecting the objectivity of this review.

ACKNOWLEDGMENTS

The authors acknowledge support from a Stanford Interdisciplinary Graduate Fellowship (to B.D.K.), National Science Foundation grant EF-2125383 (to K.C.H.), and National Institutes of Health RM1 award GM135102 (to K.C.H.). K.C.H. is a Chan Zuckerberg Biohub Investigator.

LITERATURE CITED

1. Abbondanzieri EA, Shaevitz JW, Block SM. 2005. Picocalorimetry of transcription by RNA polymerase. *Biophys. J.* 89(6):L61–63
2. Al Refaii A, Alix JH. 2009. Ribosome biogenesis is temperature-dependent and delayed in *Escherichia coli* lacking the chaperones DnaK or DnaJ. *Mol. Microbiol.* 71(3):748–62
3. Al Saleh AA. 1983. Effects of temperature on the replication of chromosomal DNA of *Xenopus laevis* cells. *J. Cell Sci.* 59:1–12
4. Almeida PFF, Vaz WLC, Thompson TE. 1992. Lateral diffusion in the liquid phases of dimyristoylphosphatidylcholine/cholesterol lipid bilayers: a free volume analysis. *Biochemistry* 31(29):6739–47
5. Anderson RL, Minton KW, Li GC, Hahn GM. 1981. Temperature-induced homeoviscous adaptation of Chinese hamster ovary cells. *Biochim. Biophys. Acta Biomembr.* 641(2):334–48
6. Araki T. 1991. The effect of temperature shifts on protein synthesis by the psychrophilic bacterium *Vibrio* sp. strain ANT-300. *J. Gen. Microbiol.* 137(4):817–26

6a. Aranda-Díaz A, Ng KM, Thomsen T, Real-Ramírez I, Dahan D, et al. 2022. Establishment and characterization of stable, diverse, fecal-derived in vitro microbial communities that model the intestinal microbiota. *Cell Host Microbe* 30(2):260–72.e5

7. Arcus VL, Mulholland AJ. 2020. Temperature, dynamics, and enzyme-catalyzed reaction rates. *Annu. Rev. Biophys.* 49:163–80
8. Arrhenius S. 1889. Über die Reaktionsgeschwindigkeit bei der Inversion von Rohrzucker durch Säuren. *Z. Phys. Chem.* 4U(1):226–48
9. Balleza E, Kim JM, Cluzel P. 2018. Systematic characterization of maturation time of fluorescent proteins in living cells. *Nat. Methods* 15(1):47–51

10. Barber MA. 1908. The rate of multiplication of *Bacillus coli* at different temperatures. *J. Infect. Dis.* 5(4):379–400
11. Bárcenas-Moreno G, Brandón MG, Rousk J, Bååth E. 2009. Adaptation of soil microbial communities to temperature: comparison of fungi and bacteria in a laboratory experiment. *Glob. Change Biol.* 15(12):2950–57
12. Bennett AF, Lenski RE, Mittler JE. 1992. Evolutionary adaptation to temperature. I. Fitness responses of *Escherichia coli* to changes in its thermal environment. *Evolution* 46(1):16–30
13. Brown HS, Licata VJ. 2013. Enthalpic switch-points and temperature dependencies of DNA binding and nucleotide incorporation by Pol I DNA polymerases. *Biochim. Biophys. Acta Proteins Proteom.* 1834(10):2133–38
14. Buckstein MH, He J, Rubin H. 2008. Characterization of nucleotide pools as a function of physiological state in *Escherichia coli*. *J. Bacteriol.* 190(2):718–26
15. Budin I, de Rond T, Chen Y, Chan LJG, Petzold CJ, Keasling JD. 2018. Viscous control of cellular respiration by membrane lipid composition. *Science* 362(6419):1186–89
16. Çaglayan M, Bilgin N. 2012. Temperature dependence of accuracy of DNA polymerase I from *Geobacillus anatolicus*. *Biochimie* 94(9):1968–73
17. Casadevall A. 2012. Fungi and the rise of mammals. *PLOS Pathog.* 8(8):e1002808
18. Cavicchioli R, Ripple WJ, Timmis KN, Azam F, Bakken LR, et al. 2019. Scientists' warning to humanity: microorganisms and climate change. *Nat. Rev. Microbiol.* 17(9):569–86
19. Chapman JD, Pollard EC. 1969. Characteristics of the enzymatic breakdown of DNA in *Escherichia coli* in response to ionizing radiation. *Int. J. Radiat. Biol.* 15(4):323–33
20. Chen K, Gao Y, Mih N, O'Brien EJ, Yang L, Palsson BO. 2017. Thermosensitivity of growth is determined by chaperone-mediated proteome reallocation. *PNAS* 114(43):11548–53
21. Chohji T, Sawada T, Kuno S. 1976. Macromolecule synthesis in *Escherichia coli* BB under various growth conditions. *Appl. Environ. Microbiol.* 31(6):864–69
22. Chrétien D, Bénit P, Ha HH, Keipert S, El-Khoury R, et al. 2018. Mitochondria are physiologically maintained at close to 50°C. *PLOS Biol.* 16(1):e2003992
23. Corkrey R, McMeekin TA, Bowman JP, Ratkowsky DA, Olley J, Ross T. 2016. The biokinetic spectrum for temperature. *PLOS ONE* 11(4):e0153343
24. Corkrey R, Olley J, Ratkowsky D, McMeekin T, Ross T. 2012. Universality of thermodynamic constants governing biological growth rates. *PLOS ONE* 7(2):e32003
25. Cossins AR, Prosser CL. 1978. Evolutionary adaptation of membranes to temperature. *PNAS* 75(4):2040–43
26. Crick FHC. 1966. Codon–anticodon pairing: the wobble hypothesis. *J. Mol. Biol.* 19(2):548–55
27. Darland G, Brock TD. 1971. *Bacillus acidocaldarius* sp. nov., an acidophilic thermophilic spore-forming bacterium. *J. Gen. Microbiol.* 67(1):9–15
28. Datta K, LiCata VJ. 2003. Thermodynamics of the binding of *Thermus aquaticus* DNA polymerase to primed-template DNA. *Nucleic Acids Res.* 31(19):5590–97
29. Datta K, Wowor AJ, Richard AJ, Licata VJ. 2006. Temperature dependence and thermodynamics of Klenow polymerase binding to primed-template DNA. *Biophys. J.* 90(5):1739–51
30. DeAngelis KM, Pold G, Topçuoglu BD, van Diepen LTA, Varney RM, et al. 2015. Long-term forest soil warming alters microbial communities in temperate forest soils. *Front. Microbiol.* 6:104
31. Deatherage DE, Kepner JL, Bennett AF, Lenski RE, Barrick JE. 2017. Specificity of genome evolution in experimental populations of *Escherichia coli* evolved at different temperatures. *PNAS* 114(10):E1904–12
32. Debey P, Hoa GHB, Douzou P, Godefroy-Colburn T, Graffe M, Grunberg-Manago M. 1975. Ribosomal subunit interaction as studied by light scattering: evidence of different classes of ribosome preparations. *Biochemistry* 14(8):1553–59
33. Dill KA, Ghosh K, Schmit JD. 2011. Physical limits of cells and proteomes. *PNAS* 108(44):17876–82
34. Dong H, Nilsson L, Kurland CG. 1996. Co-variation of tRNA abundance and codon usage in *Escherichia coli* at different growth rates. *J. Mol. Biol.* 260(5):649–63
35. Driessen RPC, Sitters G, Laurens N, Moolenaar GF, Wuite GJL, et al. 2014. Effect of temperature on the intrinsic flexibility of DNA and its interaction with architectural proteins. *Biochemistry* 53(41):6430–38

36. Duval-Valentin G, Ehrlich R. 1987. Dynamic and structural characterisation of multiple steps during complex formation between *E. coli* RNA polymerase and the tetR promoter from pSC101. *Nucleic Acids Res.* 15(2):575–94
37. Elias M, Wieczorek G, Rosenne S, Tawfik DS. 2014. The universality of enzymatic rate-temperature dependency. *Trends Biochem. Sci.* 39(1):1–7
38. Enquist BJ, Economo EP, Huxman TE, Allen AP, Ignace DD, Gillooly JF. 2003. Scaling metabolism from organisms to ecosystems. *Nature* 423(6940):639–42
39. Eyring H. 1935. The activated complex in chemical reactions. *J. Chem. Phys.* 3(2):63–71
40. Farewell A, Neidhardt FC. 1998. Effect of temperature on in vivo protein synthetic capacity in *Escherichia coli*. *J. Bacteriol.* 180(17):4704–10
41. Fehling E, Weidner M. 1986. Temperature characteristics and adaptive potential of wheat ribosomes. *Plant Physiol.* 80(1):181–86
42. Fiala KA, Sherrer SM, Brown JA, Suo Z. 2008. Mechanistic consequences of temperature on DNA polymerization catalyzed by a Y-family DNA polymerase. *Nucleic Acids Res.* 36(6):1990–2001
43. Fiil NP, von Meyenburg K, Friesen JD. 1972. Accumulation and turnover of guanosine tetraphosphate in *Escherichia coli*. *J. Mol. Biol.* 71(3):769–83
44. Fijalkowska IJ, Schaaper RM, Jonczyk P. 2012. DNA replication fidelity in *Escherichia coli*: a multi-DNA polymerase affair. *FEMS Microbiol. Rev.* 36(6):1105–21
45. Frey SD, Drijber R, Smith H, Melillo J. 2008. Microbial biomass, functional capacity, and community structure after 12 years of soil warming. *Soil Biol. Biochem.* 40(11):2904–7
46. Frieler K, Meinshausen M, Golly A, Mengel M, Lebek K, et al. 2013. Limiting global warming to 2°C is unlikely to save most coral reefs. *Nat. Clim. Change* 3(2):165–70
47. Gadgil M, Kapur V, Hu WS. 2005. Transcriptional response of *Escherichia coli* to temperature shift. *Biotechnol. Prog.* 21(3):689–99
48. Galtier N, Lobry JR. 1997. Relationships between genomic G+C content, RNA secondary structures, and optimal growth temperature in prokaryotes. *J. Mol. Evol.* 44(6):632–36
49. Gillooly JF, Brown JH, West GB, Savage VM, Charnov EL. 2001. Effects of size and temperature on metabolic rate. *Science* 293(5538):2248–51
50. Goldford JE, Lu N, Bajić D, Estrela S, Tikhonov M, et al. 2018. Emergent simplicity in microbial community assembly. *Science* 361(6401):469–74
51. Gould BS, Sizer IW. 1938. The mechanism of bacterial dehydrogenase activity in vivo. *J. Biol. Chem.* 124(1):269–79
52. Gruener N, Avi-Dor Y. 1966. Temperature-dependence of activation and inhibition of rat-brain adenosine triphosphatase activated by sodium and potassium ions. *Biochem. J.* 100(3):762–67
53. Hassan N, Anesio AM, Rafiq M, Holtvoeth J, Bull I, et al. 2020. Temperature driven membrane lipid adaptation in glacial psychrophilic bacteria. *Front. Microbiol.* 11:824
54. Herendeen SL, VanBogelen RA, Neidhardt FC. 1979. Levels of major proteins of *Escherichia coli* during growth at different temperatures. *J. Bacteriol.* 139(1):185–94
55. Herrero AA, Gomez RF. 1980. Development of ethanol tolerance in *Clostridium thermocellum*: effect of growth temperature. *Appl. Environ. Microbiol.* 40(3):571–77
56. Hinshelwood SCN. 1952. On the chemical kinetics of autosynthetic systems. *J. Chem. Soc.* 1952:745–55
57. Hoa GHB, Graffe M, Grunberg-Manago M. 1977. Thermodynamic studies of the reversible association of *Escherichia coli* ribosomal subunits. *Biochemistry* 16(12):2800–5
58. Hurst LD, Merchant AR. 2001. High guanine-cytosine content is not an adaptation to high temperature: a comparative analysis amongst prokaryotes. *Proc. R. Soc. B* 268(1466):493–97
59. Hutchins DA, Jansson JK, Remais JV, Rich VI, Singh BK, Trivedi P. 2019. Climate change microbiology—problems and perspectives. *Nat. Rev. Microbiol.* 17(6):391–96
60. Iyer-Biswas S, Wright CS, Henry JT, Lo K, Burov S, et al. 2014. Scaling laws governing stochastic growth and division of single bacterial cells. *PNAS* 111(45):15912–17
61. Jansson JK, Hofmockel KS. 2020. Soil microbiomes and climate change. *Nat. Rev. Microbiol.* 18(1):35–46
62. Johansson M, Bouakaz E, Lovmar M, Ehrenberg M. 2008. The kinetics of ribosomal peptidyl transfer revisited. *Mol. Cell* 30(5):589–98

63. Johnson RS, Chester RE. 1998. Stopped-flow kinetic analysis of the interaction of *Escherichia coli* RNA polymerase with the bacteriophage T7 A1 promoter. *J. Mol. Biol.* 283(2):353–70
64. Jurburg SD, Nunes I, Brejnrod A, Jacquiod S, Priemé A, et al. 2017. Legacy effects on the recovery of soil bacterial communities from extreme temperature perturbation. *Front. Microbiol.* 8:1832
65. Katunin VI, Savelsbergh A, Rodnina MV, Wintermeyer W. 2002. Coupling of GTP hydrolysis by elongation factor G to translocation and factor recycling on the ribosome. *Biochemistry* 41(42):12806–12
66. Kawashima T, Amano N, Koike H, Makino SI, Higuchi S, et al. 2000. Archaeal adaptation to higher temperatures revealed by genomic sequence of *Thermoplasma volcanium*. *PNAS* 97(26):14257–62
67. Knapp BD, Zhu L, Huang KC. 2020. SiCTeC: an inexpensive, easily assembled Peltier device for rapid temperature shifting during single-cell imaging. *PLOS Biol*. 18(11):e3000786
68. Köhler JR, Hube B, Puccia R, Casadevall A, Perfect JR. 2017. Fungi that infect humans. *Microbiol. Spectr.* 5(3). **https://doi.org/10.1128/microbiolspec.FUNK-0014-2016**
69. Kong H, Kucera RB, Jack WE. 1993. Characterization of a DNA polymerase from the hyperthermophile archaea *Thermococcus litoralis*: vent DNA polymerase, steady state kinetics, thermal stability, processivity, strand displacement, and exonuclease activities. *J. Biol. Chem.* 268(3):1965–75
70. Kortmann J, Narberhaus F. 2012. Bacterial RNA thermometers: molecular zippers and switches. *Nat. Rev. Microbiol.* 10(4):255–65
71. Kowalak JA, Dalluge JJ, McCloskey JA, Stetter KO. 1994. The role of posttranscriptional modification in stabilization of transfer RNA from hyperthermophiles. *Biochemistry* 33(25):7869–76
72. Kuhlenkoetter S, Wintermeyer W, Rodnina M V. 2011. Different substrate-dependent transition states in the active site of the ribosome. *Nature* 476(7360):351–54
73. Langer A, Schräml M, Strasser R, Daub H, Myers T, et al. 2015. Polymerase/DNA interactions and enzymatic activity: multi-parameter analysis with electro-switchable biosurfaces. *Sci. Rep.* 5:12066
74. LaRiviere FJ, Wolfson AD, Uhlenbeck OC. 2001. Uniform binding of aminoacyl-tRNAs to elongation factor Tu by thermodynamic compensation. *Science* 294(5540):165–68
75. Lax S, Abreu CI, Gore J. 2020. Higher temperatures generically favour slower-growing bacterial species in multispecies communities. *Nat. Ecol. Evol.* 4(4):560–67
76. Lemaux PG, Herendeen SL, Bloch PL, Neidhardt FC. 1978. Transient rates of synthesis of individual polypeptides in *E. coli* following temperature shifts. *Cell* 13(3):427–34
77. Leung EKY, Suslov N, Tuttle N, Sengupta R, Piccirilli JA. 2011. The mechanism of peptidyl transfer catalysis by the ribosome. *Annu. Rev. Biochem.* 80:527–55
78. Li G-W, Burkhardt D, Gross C, Weissman JS, Babu M, et al. 2014. Quantifying absolute protein synthesis rates reveals principles underlying allocation of cellular resources. *Cell* 157(3):624–35
79. Lindahl L. 1975. Intermediates and time kinetics of the in vivo assembly of *Escherichia coli* ribosomes. *J. Mol. Biol.* 92(1):15–37
80. Lorenz C, Lünse C, Mörl M. 2017. tRNA modifications: impact on structure and thermal adaptation. *Biomolecules* 7(4):35
81. Luláková P, Perez-Mon C, Šantrůčková H, Ruethi J, Frey B. 2019. High-alpine permafrost and active-layer soil microbiomes differ in their response to elevated temperatures. *Front. Microbiol.* 10:668
82. Luo C, Rodriguez-R LM, Johnston ER, Wu L, Cheng L, et al. 2014. Soil microbial community responses to a decade of warming as revealed by comparative metagenomics. *Appl. Environ. Microbiol.* 80(5):1777–86
83. Ma DK, Li Z, Lu AY, Sun F, Chen S, et al. 2015. Acyl-CoA dehydrogenase drives heat adaptation by sequestering fatty acids. *Cell* 161(5):1152–63
84. MacFadden DR, McGough SF, Fisman D, Santillana M, Brownstein JS. 2018. Antibiotic resistance increases with local temperature. *Nat. Clim. Change* 8(6):510–14
85. Mackow ER, Chang FN. 1983. Correlation between RNA synthesis and ppGpp content in *Escherichia coli* during temperature shifts. *Mol. Gen. Genet.* 192(1–2):5–9
86. Magnusson LU, Farewell A, Nyström T. 2005. ppGpp: a global regulator in *Escherichia coli*. *Trends Microbiol.* 13(5):236–42
87. Manor H, Goodman D, Stent GS. 1969. RNA chain growth rates in *Escherichia coli*. *J. Mol. Biol.* 39(1):1–29

88. Marr AG, Ingraham JL. 1962. Effect of temperature on the composition of fatty acids in *Escherichia coli*. *J. Bacteriol.* 84(6):1260–67
89. Marsland R, Cui W, Mehta P. 2020. A minimal model for microbial biodiversity can reproduce experimentally observed ecological patterns. *Sci. Rep.* 10:3308
90. Maslak M, Martin CT. 1993. Kinetic analysis of T7 RNA polymerase transcription initiation from promoters containing single-stranded regions. *Biochemistry* 32(16):4281–85
91. McClure WR, Cech CL. 1978. On the mechanism of rifampicin inhibition of RNA synthesis. *J. Biol. Chem.* 253(24):8949–56
92. McClure WR, Jovin TM. 1975. The steady state kinetic parameters and non-processivity of *Escherichia coli* deoxyribonucleic acid polymerase I. *J. Biol. Chem.* 250(11):4073–80
93. Melillo JM, Frey SD, DeAngelis KM, Werner WJ, Bernard MJ, et al. 2017. Long-term pattern and magnitude of soil carbon feedback to the climate system in a warming world. *Science* 358(6359):101–5
94. Melillo JM, Steudler PA, Aber JD, Newkirk K, Lux H, et al. 2002. Soil warming and carbon-cycle feedbacks to the climate system. *Science* 298(5601):2173–76
95. Michaels GA. 1972. Ribosome maturation of *Escherichia coli* growing at different growth rates. *J. Bacteriol.* 110(3):889–94
96. Miguel A, Montón F, Li T, Gómez-Herreros F, Chávez S, et al. 2013. External conditions inversely change the RNA polymerase II elongation rate and density in yeast. *Biochim. Biophys. Acta Gene Regul. Mech.* 1829(11):1248–55
97. Mihursky JA, McErlean AJ, Kennedy VS. 1970. Thermal pollution, aquaculture and pathobiology in aquatic systems. *J. Wildl. Dis.* 6(4):347–55
98. Miller M, Pedersen JZ, Cox RP. 1988. Effect of growth temperature on membrane dynamics in a thermophilic cyanobacterium: a spin label study. *Biochim. Biophys. Acta Biomembr.* 943(3):501–10
99. Mohr PW, Krawiec S. 1980. Temperature characteristics and Arrhenius plots for nominal psychrophiles, mesophiles and thermophiles. *J. Gen. Microbiol.* 121(2):311–17
100. Monod J. 1949. The growth of bacterial cultures. *Annu. Rev. Microbiol.* 3:371–94
101. Monson RK, Burns SP, Williams MW, Delany AC, Weintraub M, Lipson DA. 2006. The contribution of beneath-snow soil respiration to total ecosystem respiration in a high-elevation, subalpine forest. *Global Biogeochem. Cycles* 20(3):GB3030
102. Mykytczuk NCS, Foote SJ, Omelon CR, Southam G, Greer CW, Whyte LG. 2013. Bacterial growth at −15°C: molecular insights from the permafrost bacterium *Planococcus halocryophilus* Or1. *ISME J.* 7(6):1211–26
103. Nakashima H, Fukuchi S, Nishikawa K. 2003. Compositional changes in RNA, DNA and proteins for bacterial adaptation to higher and lower temperatures. *J. Biochem.* 133(4):507–13
104. Nguyen V, Wilson C, Hoemberger M, Stiller JB, Agafonov RV, et al. 2017. Evolutionary drivers of thermoadaptation in enzyme catalysis. *Science* 355(6322):289–94
105. Okabe K, Sakaguchi R, Shi B, Kiyonaka S. 2018. Intracellular thermometry with fluorescent sensors for thermal biology. *Pflugers Arch. Eur. J. Physiol.* 470(5):717–31
106. Oshima T, Imahori K. 1974. Description of *Thermus thermophilus* (Yoshida and Oshima) comb. nov., a nonsporulating thermophilic bacterium from a Japanese thermal spa. *Int. J. Syst. Bacteriol.* 24(1):102–12
107. Pace B, Campbell LL. 1967. Correlation of maximal growth temperature and ribosome heat stability. *PNAS* 57(4):1110–16
108. Phillips R, Kondev J, Theriot J, Garcia HG, Orme N. 2012. *Physical Biology of the Cell*. New York: Garland Science
109. Pierucci O. 1972. Chromosome replication and cell division in *Escherichia coli* at various temperatures of growth. *J. Bacteriol.* 109(2):848–54
110. Pietikäinen J, Pettersson M, Bååth E. 2005. Comparison of temperature effects on soil respiration and bacterial and fungal growth rates. *FEMS Microbiol. Ecol.* 52(1):49–58
111. Raison JK. 1973. The influence of temperature-induced phase changes on the kinetics of respiratory and other membrane-associated enzyme systems. *J. Bioenerg.* 4(1–2):285–309
112. Raison JK, Lyons JM, Mehlhorn RJ, Keith AD. 1971. Temperature-induced phase changes in mitochondrial membranes detected by spin labeling. *J. Biol. Chem.* 246(12):4036–40

113. Rao PN, Engelbero J. 1965. HeLa cells: effects of temperature on the life cycle. *Science* 38(148):1092–94
114. Ratkowsky DA, Olley J, McMeekin TA, Ball A. 1982. Relationship between temperature and growth rate of bacterial cultures. *J. Bacteriol.* 149(1):1–5
115. Richter K, Haslbeck M, Buchner J. 2010. The heat shock response: life on the verge of death. *Mol. Cell* 40(2):253–66
116. Ritchie ME. 2018. Reaction and diffusion thermodynamics explain optimal temperatures of biochemical reactions. *Sci. Rep.* 8:11105
117. Robinson JL, Pyzyna B, Atrasz RG, Henderson CA, Morrill KL, et al. 2005. Growth kinetics of extremely halophilic Archaea (family Halobacteriaceae) as revealed by Arrhenius plots. *J. Bacteriol.* 187(3):923–29
118. Rodnina MV, Pape T, Fricke R, Kuhn L, Wintermeyer W. 1996. Initial binding of the elongation factor Tu-GTP-aminoacyl-tRNA complex preceding codon recognition on the ribosome. *J. Biol. Chem.* 271(2):646–52
119. Rodriguez-Correa D, Dahlberg AE. 2008. Kinetic and thermodynamic studies of peptidyltransferase in ribosomes from the extreme thermophile *Thermus thermophilus*. *RNA* 14(11):2314–18
120. Rodríguez-Verdugo A, Carrillo-Cisneros D, González-González A, Gaut BS, Bennett AF. 2014. Different tradeoffs result from alternate genetic adaptations to a common environment. *PNAS* 111(33):12121–26
121. Roe JH, Burgess RR, Record MT. 1984. Kinetics and mechanism of the interaction of *Escherichia coli* RNA polymerase with the λPR promoter. *J. Mol. Biol.* 176(4):495–522
122. Roe JH, Burgess RR, Record MT. 1985. Temperature dependence of the rate constants of the *Escherichia coli* RNA polymerase-lambda PR promoter interaction: assignment of the kinetic steps corresponding to protein conformational change and DNA opening. *J. Mol. Biol.* 184(3):441–53
123. Roszak DB, Colwell RR. 1987. Survival strategies of bacteria in the natural environment. *Microbiol. Rev.* 51(3):365–79
124. Rudolph B, Gebendorfer KM, Buchner J, Winter J. 2010. Evolution of *Escherichia coli* for growth at high temperatures. *J. Biol. Chem.* 285(25):19029–34
125. Ryals J, Little R, Bremer H. 1982. Temperature dependence of RNA synthesis parameters in *Escherichia coli*. *J. Bacteriol.* 151(2):879–87
126. Saladino CF, Johnson HA. 1974. Rate of DNA synthesis as a function of temperature in cultured hamster fibroblasts (V-79) and HeLa-S3 cells. *Exp. Cell Res.* 85(2):248–54
127. Satapathy SS, Dutta M, Ray SK. 2010. Higher tRNA diversity in thermophilic bacteria: a possible adaptation to growth at high temperature. *Microbiol. Res.* 165(8):609–16
128. Satapathy SS, Dutta M, Ray SK. 2010. Variable correlation of genome GC% with transfer RNA number as well as with transfer RNA diversity among bacterial groups: α-proteobacteria and Tenericutes exhibit strong positive correlation. *Microbiol. Res.* 165(3):232–42
129. Sawle L, Ghosh K. 2011. How do thermophilic proteins and proteomes withstand high temperature? *Biophys. J.* 101(1):217–27
130. Scalley ML, Baker D. 1997. Protein folding kinetics exhibit an Arrhenius temperature dependence when corrected for the temperature dependence of protein stability. *PNAS* 94(20):10636–40
131. Schaechter M, Maaloe O, Kjeldgaard NO. 1958. Dependency on medium and temperature of cell size and chemical composition during balanced growth of *Salmonella typhimurium*. *J. Gen. Microbiol.* 19(3):592–606
132. Scholtissek C, Rott R. 1969. Effect of temperature on the multiplication of an influenza virus. *J. Gen. Virol.* 5(2):283–90
133. Schroeder GK, Wolfenden R. 2007. The rate enhancement produced by the ribosome: an improved model. *Biochemistry* 46(13):4037–44
134. Scott M, Mateescu EM, Zhang Z, Hwa T. 2010. Interdependence of cell growth origins and consequences. *Science* 330(6007):1099–102
135. Seeton CJ. 2006. Viscosity-temperature correlation for liquids. *Tribol. Lett.* 22(1):67–78
136. Sells BH, Davis FC. 1968. Ribosome biogenesis: nonrandom addition of structural proteins to 50S subunits. *Science* 159(3820):1240–42
137. Shajani Z, Sykes MT, Williamson JR. 2011. Assembly of bacterial ribosomes. *Annu. Rev. Biochem.* 80:501–26

138. Sievers A, Beringer M, Rodnina MV, Wolfenden R. 2004. The ribosome as an entropy trap. *PNAS* 101(21):7897–901
139. Siliakus MF, van der Oost J, Kengen SWM. 2017. Adaptations of archaeal and bacterial membranes to variations in temperature, pH and pressure. *Extremophiles* 21(4):651–70
140. Sinensky M. 1974. Homeoviscous adaptation: a homeostatic process that regulates the viscosity of membrane lipids in *Escherichia coli*. *PNAS* 71(2):522–25
141. Sizer IW. 1943. Effects of temperature on enzyme kinetics. In *Advances in Enzymology and Related Areas of Molecular Biology*, Vol. 3, ed. FF Nord, CH Werkman, pp. 35–62. New York: Wiley
142. Solage A, Cedar H. 1976. The kinetics of *E. coli* RNA polymerase. *Nucleic Acids Res*. 3(9):2207–22
143. Spencer-Martins I, Van Uden N. 1982. The temperature profile of growth, death and yield of the starch-converting yeast *Lipomyces kononenkoae*. *Z. Allg. Mikrobiol.* 22(7):503–5
144. Sunagawa S, Coelho LP, Chaffron S, Kultima JR, Labadie K, et al. 2015. Structure and function of the global ocean microbiome. *Science* 348(6237):1261359
145. Sykes J, Young TW. 1968. Studies on the ribosomes and ribonucleic acids of *Aerobacter aerogenes* grown at different rates in carbon-limited continuous culture. *Biochim. Biophys. Acta Nucleic Acids Protein Synth.* 169(1):103–16
146. Tagkopoulos I, Liu Y-C, Tavazoie S. 2008. Predictive behavior within microbial genetic networks. *Science* 320(5881):1313–17
147. Talkington MWT, Siuzdak G, Williamson JR. 2005. An assembly landscape for the 30S ribosomal subunit. *Nature* 438(7068):628–32
148. Tenaillon O, Rodríguez-Verdugo A, Gaut RL, McDonald P, Bennett AF, et al. 2012. The molecular diversity of adaptive convergence. *Science* 335(6067):457–61
149. Thompson MC, Barad BA, Wolff AM, Sun Cho H, Schotte F, et al. 2019. Temperature-jump solution X-ray scattering reveals distinct motions in a dynamic enzyme. *Nat. Chem.* 11(11):1058–66
150. Towers NR, Raison JK, Kellerman GM, Linnane AW. 1972. Effects of temperature-induced phase changes in membranes on protein synthesis by bound ribosomes. *Biochim. Biophys. Acta Nucleic Acids Protein Synth.* 287(2):301–11
151. Trgovčevic Ž, Kucan Ž. 1970. Is DNA polymerase involved in DNA degradation following ionizing radiation? *Nature* 226(5247):752–53
152. Újvári A, Martin CT. 1996. Thermodynamic and kinetic measurements of promoter binding by T7 RNA polymerase. *Biochemistry* 35(46):14574–82
153. Uma S, Jadhav RS, Seshu Kumar G, Shivaji S, Ray MK. 1999. A RNA polymerase with transcriptional activity at 0°C from the Antarctic bacterium *Pseudomonas syringae*. *FEBS Lett.* 453(3):313–17
154. Van De Vossenberg JLCM, Ubbink-Kok T, Elferink MGL, Driessen AJM, Konings WN. 1995. Ion permeability of the cytoplasmic membrane limits the maximum growth temperature of bacteria and archaea. *Mol. Microbiol.* 18(5):925–32
155. VanBogelen RA, Neidhardt FC. 1990. Ribosomes as sensors of heat and cold shock in *Escherichia coli*. *PNAS* 87(15):5589–93
156. Vanoni M, Vai M, Frascotti G. 1984. Effects of temperature on the yeast cell cycle analyzed by flow cytometry. *Cytometry* 5(5):530–33
157. Voges MJEEE, Bai Y, Schulze-Lefert P, Sattely ES. 2019. Plant-derived coumarins shape the composition of an *Arabidopsis* synthetic root microbiome. *PNAS* 116(25):12558–65
158. Waldron C, Lacroute F. 1975. Effect of growth rate on the amounts of ribosomal and transfer ribonucleic acids in yeast. *J. Bacteriol.* 122(3):855–65
159. Walter G, Zillig W, Palm P, Fuchs E. 1967. Initiation of DNA-dependent RNA synthesis and the effect of heparin on RNA polymerase. *Eur. J. Biochem.* 3(2):194–201
160. Watanabe I, Okada S. 1967. Effects of temperature on growth rate of cultured mammalian cells (L5178Y). *J. Cell Biol.* 32(2):309–23
161. Watanabe K, Shinma M, Oshima T, Nishimura S. 1976. Heat-induced stability of tRNA from an extreme thermophile, *Thermus thermophilus*. *Biochem. Biophys. Res. Commun.* 72(3):1137–44
162. Whitrow M. 1990. Wagner-Jauregg and fever therapy. *Med. Hist.* 34(3):294–310
163. Wolfenden R, Snider M, Ridgway C, Miller B. 1999. The temperature dependence of enzyme rate enhancements. *J. Am. Chem. Soc.* 121(32):7419–20

164. Wowor AJ, Datta K, Brown HS, Thompson GS, Ray S, et al. 2010. Thermodynamics of the DNA structural selectivity of the Pol I DNA polymerases from *Escherichia coli* and *Thermus aquaticus*. *Biophys. J.* 98(12):3015–24
165. Yergeau E, Kowalchuk GA. 2008. Responses of Antarctic soil microbial communities and associated functions to temperature and freeze-thaw cycle frequency. *Environ. Microbiol.* 10(9):2223–35
166. Zakim D, Kavecansky J, Scarlata S. 1992. Are membrane enzymes regulated by the viscosity of the membrane environment? *Biochemistry* 31(46):11589–94
167. Zaritsky A. 1982. Effects of growth temperature on ribosomes and other physiological properties of *Escherichia coli*. *J. Bacteriol.* 151(1):485–86
168. Zhu M, Dai X. 2019. Growth suppression by altered (p)ppGpp levels results from non-optimal resource allocation in *Escherichia coli*. *Nucleic Acids Res.* 47(9):4684–93

Annual Review of Biophysics
Volume 51, 2022

Contents

Indexes

Errata

An online log of corrections to *Annual Review of Biophysics* articles may be found at http://www.annualreviews.org/errata/biophys